

DEPARTMENT OF TRANSPORTATION REPORT NO. 31.1

PHOTOGRAMMETRIC MONITORING OF A GABION WALL

Research Project

Y-1699

September 1977

S. A. Veress, D.Sc.  
E. E. Flint, M.S. L. L. Sun, M.S. John Hatzopoulos, M.S.  
and C. Jinina, Graduate Student

Prepared for  
Washington State Highway Commission

in cooperation with  
U. S. Department of Transportation  
Federal Highway Administration

UNIVERSITY OF WASHINGTON  
College of Engineering  
DEPARTMENT OF CIVIL ENGINEERING

PHOTOGRAMMETRIC MONITORING  
OF A GABION WALL

Final Technical Report  
Research Report  
1977

Prepared by

S. A. Veress D.Sc., Principal Investigator  
M. C. Y. Hou Ph.D., Research Assistant Professor  
E. E. Flint M.S., Research Assistant  
L. L. Sun M.S., Research Assistant  
J. N. Hatzopoulos M.S., Research Assistant  
and  
C. Jijina, Graduate Student

Research conducted for Washington State Highway Commission, Department of Highways, in cooperation with U.S. Department of Transportation - Federal Highway Administration, under Agreement No. Y-1699.

The opinions, findings and conclusions expressed in this publication are those of the authors and not necessarily those of the Washington State Highway Department or Federal Highway Administration.

1. Report No. D.O.T. Report No. 31.1		2. Government Accession No.		3. Recipient's Catalog No.	
4. Title and Subtitle PHOTOGRAMMETRIC MONITORING OF A GABION WALL				5. Report Date 9/1977	
				6. Performing Organization Code	
7. Author(s) S. A. Veress, M. C. Y. Hou, E. E. Flint, L. L. Sun, J. N. Hatzopoulos, and C. Jijina				8. Performing Organization Report No.	
9. Performing Organization Name and Address Civil Engineering Department, University of Washington, Seattle, Washington 98195				10. Work Unit No.	
				11. Contract or Grant No. Y-1699	
12. Sponsoring Agency Name and Address Washington State Highway Commission, Department of Highways, Highway Administration Building, Olympia, Washington 98504				13. Type of Report and Period Covered Final Technical Report	
				14. Sponsoring Agency Code	
15. Supplementary Notes This study was conducted in cooperation with the U. S. Department of Transportation, Federal Highway Administration					
16. Abstract A photogrammetric monitoring method of structural deformation has been developed during the course of this project. The Gabion Wall which is part of the I-90 project has been used as the site for practical tests of the theoretical development. The monitoring consists of photographing the structure from three camera stations with KA-2 f=24" camera. The camera has been modified to a plate camera to provide the maximum accuracy. The methodology consists of the geodetic determination of the camera location and the orientation and photogrammetric determination of targets (natural and artificial) on the structure. During the course of this project more than 100 target locations were determined by three dimensional coordinates. The maximum error was found to be + 3/4 inch; the average, 1/2 inch. This represents a relative accuracy of from 1/58,000 to 1/120,000 of the photographic distance. Using the actual construction site for research has permitted immediate implementation. The instrumentation as well as the methodology along with the computer program has been transmitted to the Washington State Highway Department and their Photogrammetric Branch has been assisted in the implementation.					
17. Key Words Photogrammetry, Gabion Wall, deflection, camera stations, orientation matrices, space intersection, space resection,			18. Distribution Statement No restrictions. This document is available to the public through the National Technical Information Service, Springfield, Virginia 22161.		
19. Security Classif. (of this report) Unclassified		20. Security Classif. (of this page) Unclassified		21. No. of Pages 73	22. Price

## TABLE OF CONTENTS

	page
SUMMARY . . . . .	iv
INTRODUCTION. . . . .	1
1.0 BACKGROUND STUDIES . . . . .	2
1.1 The 1968 Research. . . . .	2
1.2 Studies Outside of the U.S.A.. . . . .	3
1.3 Corps of Engineers Research. . . . .	4
1.4 The New Approach . . . . .	5
2.0 INSTRUMENTAL PROBLEMS OF MONITORING. . . . .	6
2.1 Existing Instrument. . . . .	6
2.2 KA-2 Fairchild Camera Modification and Calibration . . . . .	9
3.0 DESIGN OF PHOTOGRAMMETRIC SURVEY . . . . .	13
3.1 Design of Camera Stations. . . . .	13
3.2 Target Design. . . . .	20
3.3 Base Line and Control Net Measurement and Adjustment . . . . .	24
4.0 FUNDAMENTAL QUANTITIES FOR MONITORING. . . . .	27
4.1 Coordinates of Frontal Nodal Points. . . . .	27
4.2 Orientation of Camera Stations . . . . .	31
4.3 Data Collection. . . . .	36
4.4 Data Reduction . . . . .	38
5.0 RESULTS AND ANALYSIS . . . . .	39
5.1 Data Output and Interpretation . . . . .	39
5.2 Stability of Orientation Matrices. . . . .	45
5.3 Accuracy and Correlation of Parameters . . . . .	52
5.4 Conclusions and Recommendations. . . . .	58
6.0 REFERENCES . . . . .	62

## LIST OF FIGURES

1. General Flow Diagram of the Method . . . . .	7
2. Determination of Eccentricity Constant . . . . .	.11
3. Collimation Mark Shown on 1/4 of the Photograph of the Gabion Wall. . . . .	.14
4. Area Topographic Map . . . . .	.15
5. Cross-Sectional View of Camera Station CS 2 and Mount. . . . .	.19
6. Convergent Photography . . . . .	.22
7. Adjustment of Camera Stations. . . . .	.25
8. Coordinate of Frontal Nodal Point at Camera Station One. . . . .	.29
9. Coordinate of Frontal Nodal Point at Camera Station Three. . . . .	.30
10. Coordinates of Frontal Nodal Point at Camera Station Two . . . . .	.32
11. Deflection of Points 41 & 42 . . . . .	.47
12. Variation in $\phi$ Angle . . . . .	.53
13. Deviation in Coordinates of Control Point 993. . . . .	.55
14. Comparison of Parameters . . . . .	.57

LIST OF TABLES

	page
1. Comparison of Base Line Measurements . . . . .	27
2. The Relation of Camera Station Coordinates with Frontal Points .	33
3. List of Photogrammetrically Monitored Points . . . . .	40
4. A Sample of the Data Output. . . . .	44
5. Diations of the DZ Coordinate. . . . .	46
6. Variation of $\phi$ Angle at Station CS 1 . . . . .	49
7. Variation of $\omega$ Angle at Station CS 1 . . . . .	49
8. Variation of $\kappa$ Angle at Station CS 1 . . . . .	50
9. Variation of $\phi$ Angle at Station CS 3 . . . . .	50
10. Variation of $\omega$ Angle at Station CS 3 . . . . .	51
11. Variation of $\kappa$ Angle at Station CS 3 . . . . .	51

## SUMMARY

The Washington State Highway Department in cooperation with the Federal Highway Administration sponsored a research project to develop and implement a photogrammetric method to monitor structures. The project was performed on the Gabion Wall which is an integral part of the I-90 Interstate Highway System under construction.

The project employed three terrestrial camera stations from which the wall could be monitored. The stations were placed about 3,000 feet from the wall. A complete monitoring method had been developed which required a long focal length camera. Such a terrestrial camera is not available on the market, therefore, a KA-2 aerial camera was modified by fabricating plate holder and magazines along with camera mounts for this purpose.

Artificial and natural targets, totaling 96 points, were selected on the wall. Their positions were monitored in three dimensional space.

The accuracy and reliability of the method were checked by control points placed on bedrock a certain distance from the wall. The locations of these points were selected so that each position remained the same during the two year period. Consequently, the measurements made on them were used as a measure of achievable accuracy.

In conclusion it was found that the photogrammetric method is capable of providing spacial position of targets with high accuracy. The relative accuracy ranged from 1/50,000 to 1/150,000 of the photographic distance. The maximum error was found to be 3/4 inch in the



coordinates of the targets placed on the wall.

The advantage of the system is that the cameras are located remotely from the wall and thus, they are not disturbed by the construction vibrations, etc. The method is an external surface monitoring method. Cost analysis indicates that this is the most economical method presently known, measured in terms of \$/monitored point. Due to the fact that a rather large number of points is monitored, a statistical analysis is possible which is valuable from a theoretical point of view. Finally the method by its very nature is such that not only points but shape of structures or parts of it, such as cables, can be monitored which further makes the method unique and universal.

The data acquisition of the project was obtained at the construction site. The data reduction was done partially at the University of Washington, Department of Civil Engineering, and partially at the Photogrammetry Branch of the Washington State Highway Department. The reduced data was immediately transferred to the Construction and Material Laboratory of the Washington State Highway Department. Further, the computer programs and instrumental observations have been transferred to the Photogrammetric Branch of the Washington State Highway Department. This form of research organization permitted an immediate implementation which was regarded as the most efficient organization of the project and which could only be accomplished with strong cooperation between the Washington State Highway Department and the University of Washington.

FINAL TECHNICAL REPORT  
GABION WALL

INTRODUCTION

The general need for monitoring large structures is well known to engineers as well as to the general public. Present methods of detecting and monitoring structural deformations, motions of slide areas, etc. can be divided into two basic groups: internal and external.

Internal or subsurface methods generally utilize sophisticated instruments such as extensometers, inclinometers, strain gauges, rock noise listening devices, settlement monuments, etc. The common characteristics of most of these devices are that they provide no more than one or two dimensional information and that they must be installed during construction. These instruments are reliable and relatively accurate. However, some of them are expensive to maintain and are not independent from the structure itself and a large amount of data supplied by them is difficult to interpret.

Because of these problems, the internal monitoring systems must be accompanied by external monitoring methods. The external monitoring system consists of classical triangulation of targets along the structure with accompanying measurements by conventional or electronic survey. If there are large numbers of targets placed on the surface of the structure, the conventional survey is time consuming and expensive because it is point dependent.

The Washington State Highway Department in conjunction with the Federal Highway Administration sponsored this research project which utilized photogrammetric monitoring in conjunction with the construc-

tion of the Gabion Wall. The wall is being built in the Snoqualmie Pass area as a structural element for the planned west bound lanes of the Interstate 90 System.

The importance of this project is that photogrammetry was utilized on one of the largest gabion walls in the U.S.A. and that the research was executed parallel with the construction. The most important fact of all is that there are several internal instruments built into the wall which can independently verify the results obtained by the photogrammetric method.

### 1.0 BACKGROUND STUDIES

#### 1.1 The 1968 Research

The first research to use photogrammetry for monitoring large structures was sponsored by the Washington State Highway Department in cooperation with the U.S. Department of Transportation, Federal Highway Administration under agreement No. Y-1155 in 1968. The purpose of this research was to determine whether or not motion and deflection of a retaining wall could be determined by photogrammetric means. Terrestrial photogrammetry, using a small size photo theodolite for data acquisition, was utilized during the project.

The project was executed on a simulated retaining wall. Several methods were examined and the analytical photogrammetric method achieved the best accuracy. The residual error of the coordinates of the targets was found to be  $\pm 0.03''$  to  $\pm 0.04''$  from the photographic distance of 100 to 125 feet. This represents 1/40,000 accuracy.

The analytical method was based on space resection using the collinearity equations. This required four control points to be known on the structure. The final computational step was space intersection as a means of determining the coordinates of the targets which were mounted on the surface of the retaining wall.

Because of these achieved results and the very favorable economy, it was recommended for implementation.

### 1.2 Studies outside of the U.S.A.

The published reports and related technical articles initiated a number of organizations to undertake studies in this field of photogrammetric application. One of the most important was done by Erez in 1971. His project was performed for Hydro Quebec on the "Barage de la Loutre" Dam. He used a photogrammetric method which was similar to that of the 1968 research. However, his measurement of the field control and instrumentation were different. He used a Wild P-30 phototheodolite for the measurement of control points as well as to take the photographs of 110 targeted points located on the surface of the dam. His achieved accuracy was 1/11000. A detailed study of his work reveals that the major problem was the weak geometry of the control survey as well as the photogrammetric survey. This resulted in decreased accuracy and emphasized the importance of the geometrical considerations in the design of a monitored project.

In West Germany, Planicka used terrestrial photogrammetry for the measurement of deformation of the Steinschütt Dam. In 1972 in Rumania Gutu measured cracks in wall pillars in a salt mine using

terrestrial photogrammetry.

There are a number of other countries where photogrammetry was utilized for structural measurements. These studies however utilized the more classical approach which resulted in accuracy which may not be acceptable for most modern standards.

### 1.3 U.S. Corps of Engineers' Research

In 1970 the U.S. Army Corps of Engineers, Seattle District, realized the practical and economical potential of analytical photogrammetry as applied to monitoring structural deformations and instituted several projects under General Investigation Studies.

Photographs were taken by a modified Wild BC-4 ballastic camera with a 305 mm (12") focal length, f 2.8 Astrotar lens. The ballastic camera was modified to a phototheodolite capable of measuring horizontal and vertical angles with an accuracy of  $\pm 0.5''$  of arc. Convergent photographs were taken of the structure from three to five camera stations. These photographs were taken with 100% overlap. The novelty of their method was the simultaneous adjustment of ground survey (horizontal and vertical angles and base lines) with the photogrammetric data (photo coordinates). This method established a very flexible system with increased accuracy. The achieved accuracy ranged from 1/50,000 to 1/94,000 of the photographic distance. A disadvantage of the method is that it is necessary to solve a large number of equations simultaneously. Thus a large capacity computer is required. The major drawback, however, is the heavy weight of the instrument whose transportation weight is more than 650 pounds. This restricts

the selection of camera stations to those places which are approachable by motor vehicle.

#### 1.4 The New Approach

The Gabion Wall project was specifically designed so that large structures could be continuously monitored from long photographic distances, such as over 1,000 feet. In this particular case, the distance was about 3,000 feet. The monitoring time of the Gabion Wall has been extended to four years. During this period, the wall has been monitored while under construction by the University of Washington and it will continue to be monitored after construction by the Washington State Highway Department. The technology of this monitoring method has been transferred to the Photographic Section of the Washington State Highway Department.

There are basic differences in concept, instrumentation, and methodology of this project from the previously used methods. The approach of this method was to provide the engineer in practice with a photogrammetric monitoring method having the following criterions:

1. It should be capable of achieving the required accuracy.  
(In the case of the retaining wall the deviation should range from 0 to about 1".)
2. It should be able to be used by an experienced photogrammetrist without new basic training.
3. It should be able to provide the results within a minimum of time.
4. It should be cost effective.

A new method was designed to fulfill these requirements. The general outline of the new method is given in the flow diagram in Figure 1. The method consists of two phases, the design phase and the routine data acquisition and reduction phase.

The Design Phase has to be established only at the beginning of the project. The data acquisition and reduction must be performed for each occasion of monitoring.

The advantage of the permanent camera stations is that they do not need to be determined each time when the photographs are taken. Thus the field work is reduced by 60% as compared to the previous methods (U.S. Corps of Engineers or the Hydro-Quebec, for examples).

The data reduction consists of a vector method which provides a better accuracy for narrow angle cameras than the previously described collinearity condition. The determination of the targets is done by individual adjustment of points. Thus a mistaken datum of a point is not transferred to other points as in the case of simultaneous adjustment. In case of mistaken data the points in question can be rejected without recomputing the complete data.

All these steps are designed to provide data within a minimum amount of time. It is believed that the system is capable of doing this within 24-48 hours.

## 2.0 INSTRUMENTAL PROBLEMS OF MONITORING

### 2.1 Existing Instrument

Photogrammetric monitoring is a very recent application of the photogrammetric science to this field of engineering. As a consequence there is no photographic camera on the market which would be completely

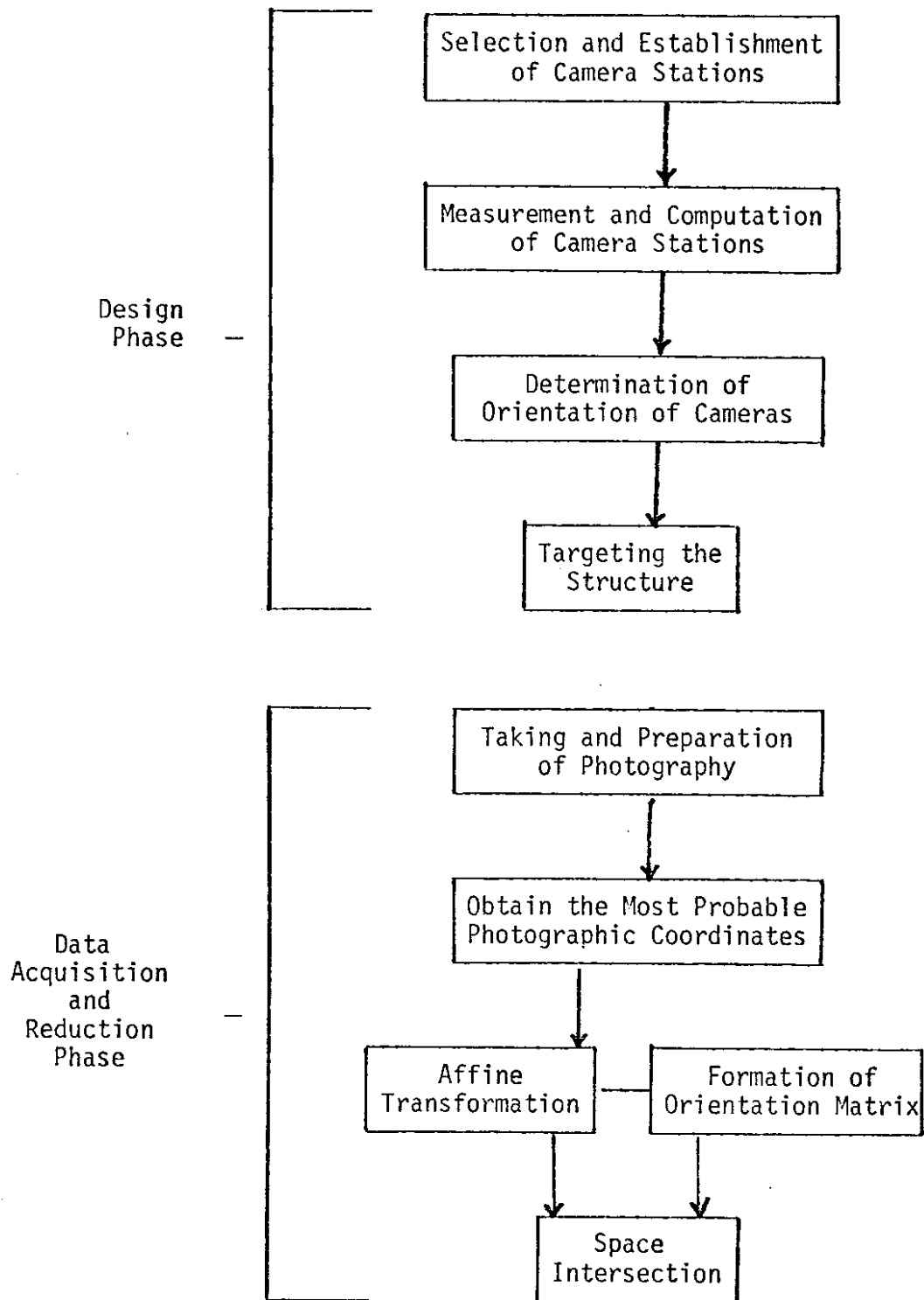


Figure 1

General Flow Diagram of the Method



suitable for monitoring purposes.

There are a number of cameras on the market which may be used, however, none of these is designed for monitoring large structures over long photographic distances.

One camera which may be used is the Wild P-31,  $f=200$  mm, format size  $83 \times 116$  mm (\$14,000). Another which would be suitable is the Janoptic Jena GmbH UMK 10/1318 terrestrial camera,  $f=100$  mm, format size  $130 \times 180$  mm (\$16,000).

Other cameras are designed for shorter distances and thus, are not suitable for this long range purpose. The Galileo Corporation of America manufactures cameras for individual order but the price of this, and as shown, of other instruments is such that the cost effectiveness of the photogrammetric monitoring is affected unfavorably and in some cases is questionable.

For these reasons it was decided that an existing aerial camera would be modified to make it suitable for this long-range purpose. To obtain the required accuracy, a Fairchild KA-2,  $f=610$  mm (24"), format size  $230 \times 230$  mm (9"x9") was modified (\$2,500). This camera was selected because of the following considerations:

1. The format size is suitable for any conventional stereoscopic plotters which are used as comparators.
2. There is no camera on the market with  $f=610$  mm (24") to provide the desired scale of photograph for more than 1,000 m or more than 3,000 ft. of photographic distance.
3. The weight of the camera is in excess of 80 pounds but it

remains portable by human means. Thus it provides more flexibility for the selection of photogrammetric geometry.

4. Last, but not least, the cost of the camera is very reasonable and the monitoring became cost effective, particularly because the camera can be used as an aerial or terrestrial camera because the film magazine is available for it.

## 2.2 KA-2 Camera Modification and Calibration

Technical data of the KA-2 camera without modification are as follows:

Focal Length:	615 mm
Format Size:	230 mm x 230 mm
Lens:	Fairchild f/6.0
Shutter Type:	3.5 Rapidyne (Day) Double Action Intra Lens
Shutter Speeds:	1/25 - 1/400 of one second
Recycle Time:	0.55 (Sec.)
Electrical Requirement:	28 V. DC/400 V. AC
Angle of View:	21° 14' by 21° 14'

Technical data of the modified camera:

Focal Length:	614.055 mm
Format Size:	230 mm x 230 mm (Plates)
Lens:	Same as Above
Shutter:	Same as Above
Shutter Speeds:	Position 1 Open 2 1/250 sec.

Shutter Speeds Continued: Position 3 1/250 sec.

4 1/60 sec.

5 1/30 sec.

6 1/15 sec.

7 1/8 sec.

Electrical Requirement: 28 V. DC

Angle of View: Same as Above

The modification consisted of:

1. Camera back for plate magazines with spring pressure
2. Shutter speed changes
3. Plate magazine constructions (10)
4. Camera suspension system
5. Collimation mark installation

The general outline of these modifications is shown in Figure 2.

The KA-2 camera is equipped with diaphragm settings ranging from f/6, f/8, f/11, f/16, to f/22. In order to insure proper exposure of the Kodak spectroscopic plates, Type IV-F, aperture shutter speeds from 1/250 to 1/8 second are necessary.

The calibration of the camera was performed by the U.S. Geological Survey, Branch of Research and Design, Reston, Virginia. The report (U.S.G.S. Report RT-R/235) has been transmitted to the Washington State Highway Department. Therefore, it will be omitted from here.

In order to (1) reduce the effect of atmospheric haze and (2) protect the lens from dust, a yellow filter which is suitable for the

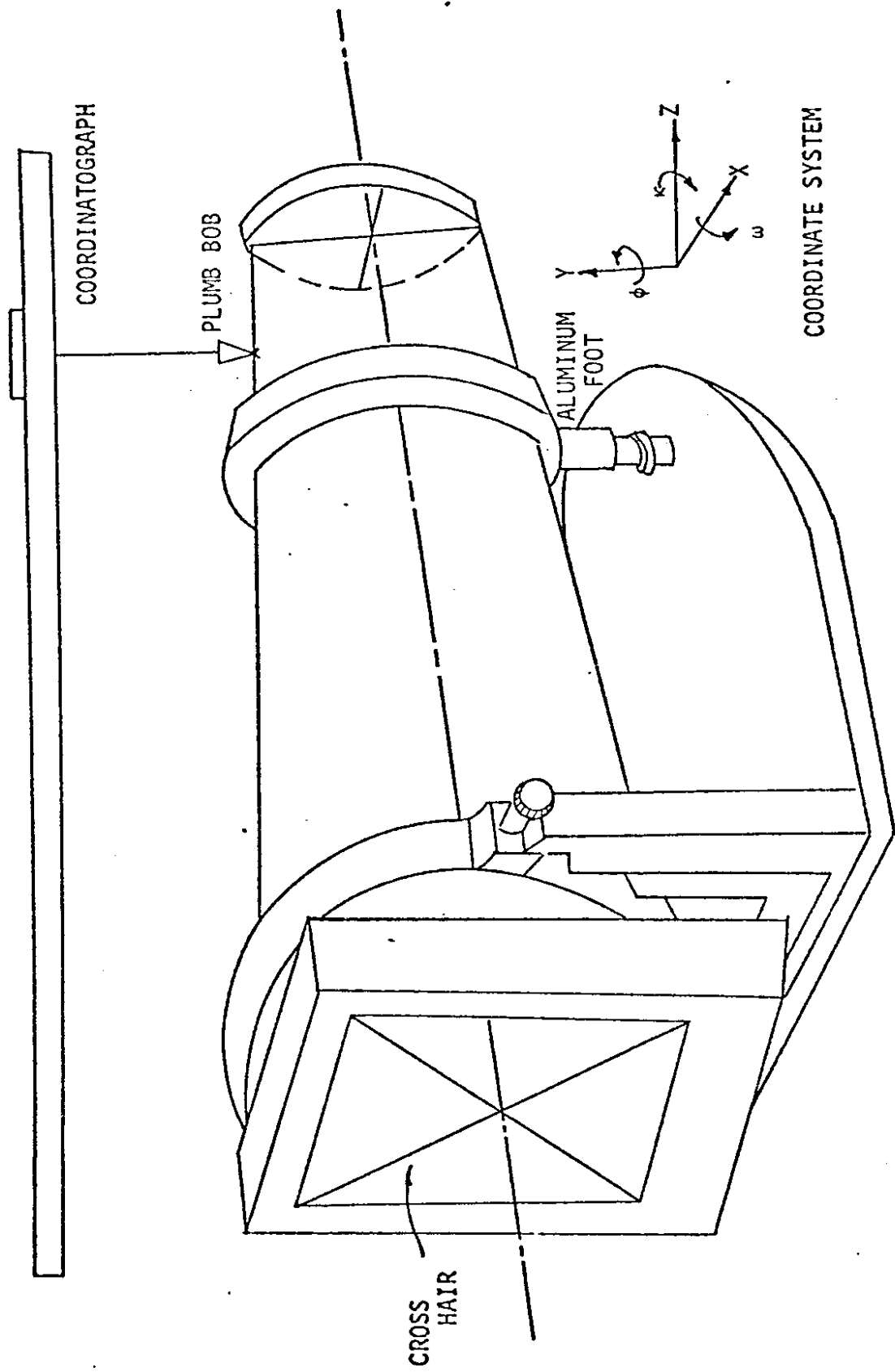


Figure 2  
 Determination of Eccentricity Constant

Gabion Wall landscapes, snow and cloudy sky, was used. The interior and exterior surfaces of the yellow filter accompanying this camera are within 80 seconds of being parallel. This filter was used for the calibration with the orientation indicated by red dots placed on the filter and camera lens. The orientation of the red dot will precisely fix the focal length value.

This calibration provided the conventional quantities used for the aerial camera. For terrestrial purposes, however, the location of frontal nodal point also had to be determined. This part of the calibration was executed at the University of Washington. The following method was used:

The camera was set under the coordinatograph bar (see Figure 2) with the plumb bob marking the precise focal length. This kind of suspension leads to an accurate exterior determination of the front nodal point which can be calibrated by the following procedure. "Line In" procedures dictate that the principle line must be centered at the camera cone ( $\phi = 0$ ). Due to the cone being slightly out-of-round, the cross-hair used to define the line of sight ordinarily consists of a vertical and horizontal hair fastened to the edge of the camera cone.

"Leveling" is effective by a boss on the bottom side securing a screwed-in aluminum foot that can be used to adjust the principle line in the y direction. A hand level ensures the principle line will be horizontal ( $\omega = 0$ ). Since the calibration, the focal length is in the "Z" direction and the  $\kappa$  rotation has little effect on measurement. The coordinatograph reading, indicated by the plumb bob, is determined by first observing the position of the vernier index on the scale to

the nearest inch. The vernier reading is then measured to one-thousandth of an inch. As a check against possible mistakes, the vernier was used to estimate the fractional part of the main-scale division by reading the index directly. Three independent determinations of the front nodal point were performed as a check for any error in measurement, thus improving the accuracy of the reading.

The installed collimation marks, one of which is shown by Figure 3, utilized the natural light entering the camera during the exposure of the photographs. This solution is adequate during good weather and terrain conditions, but in some cases the marks may not be visible and thus measurable on the photographs. Because of this reason, during this research, the collimation marks were modified by attaching light (green) emitting diodes to them. They thereby become illuminated marks which are independent of any other condition.

### 3.0 DESIGN OF PHOTOGRAMMETRIC SURVEY

The general outline of the area with relation to the Gabion Wall is given by Figure 4. The camera stations are nearly on a straight line along the present Temporary I-90 Highway. This is a very narrow piece of land which results in an ill conditioned geometry.

#### 3.1 Design of Camera Stations

As already stated earlier and as shown by Figure 2, the KA-2 camera has been modified by the addition of both fore and aft support rings mounted so that the camera is essentially balanced equally at three points: two points aft and one point forward. Through this kind of suspension the camera is balanced with the effect that swing-

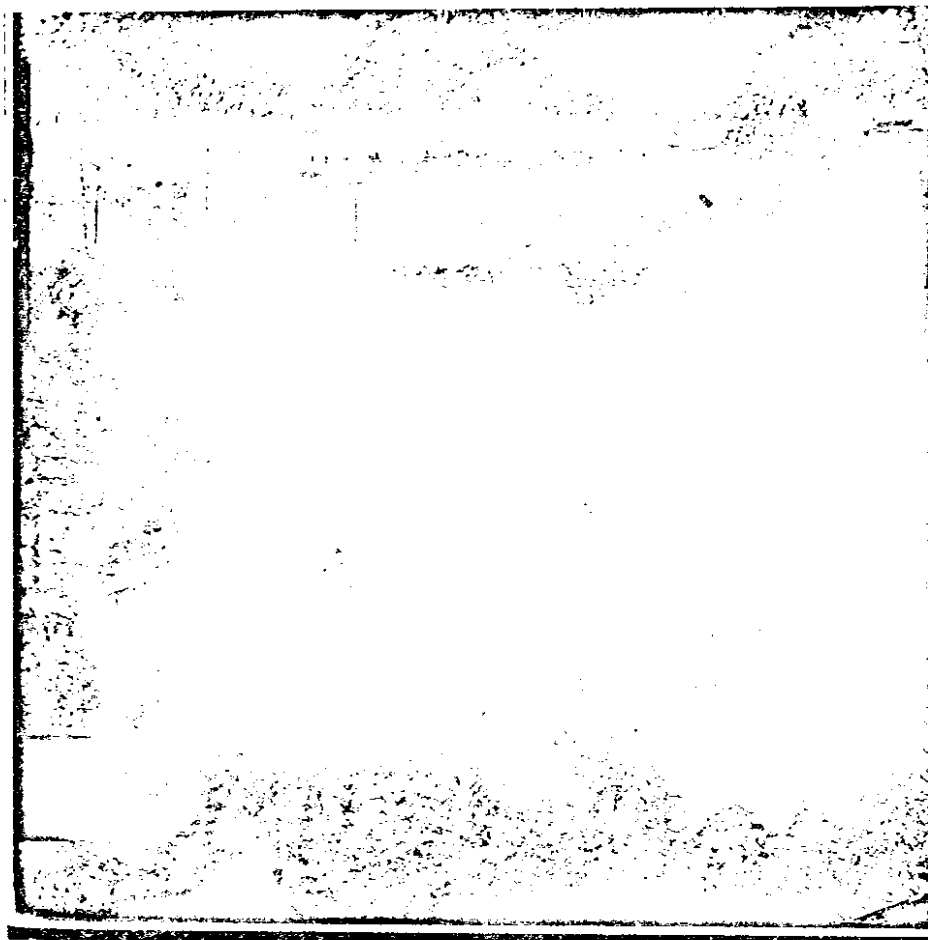


Figure 3  
Collimation Mark Shown on 1/4  
of the Photograph of the Gabion Wall

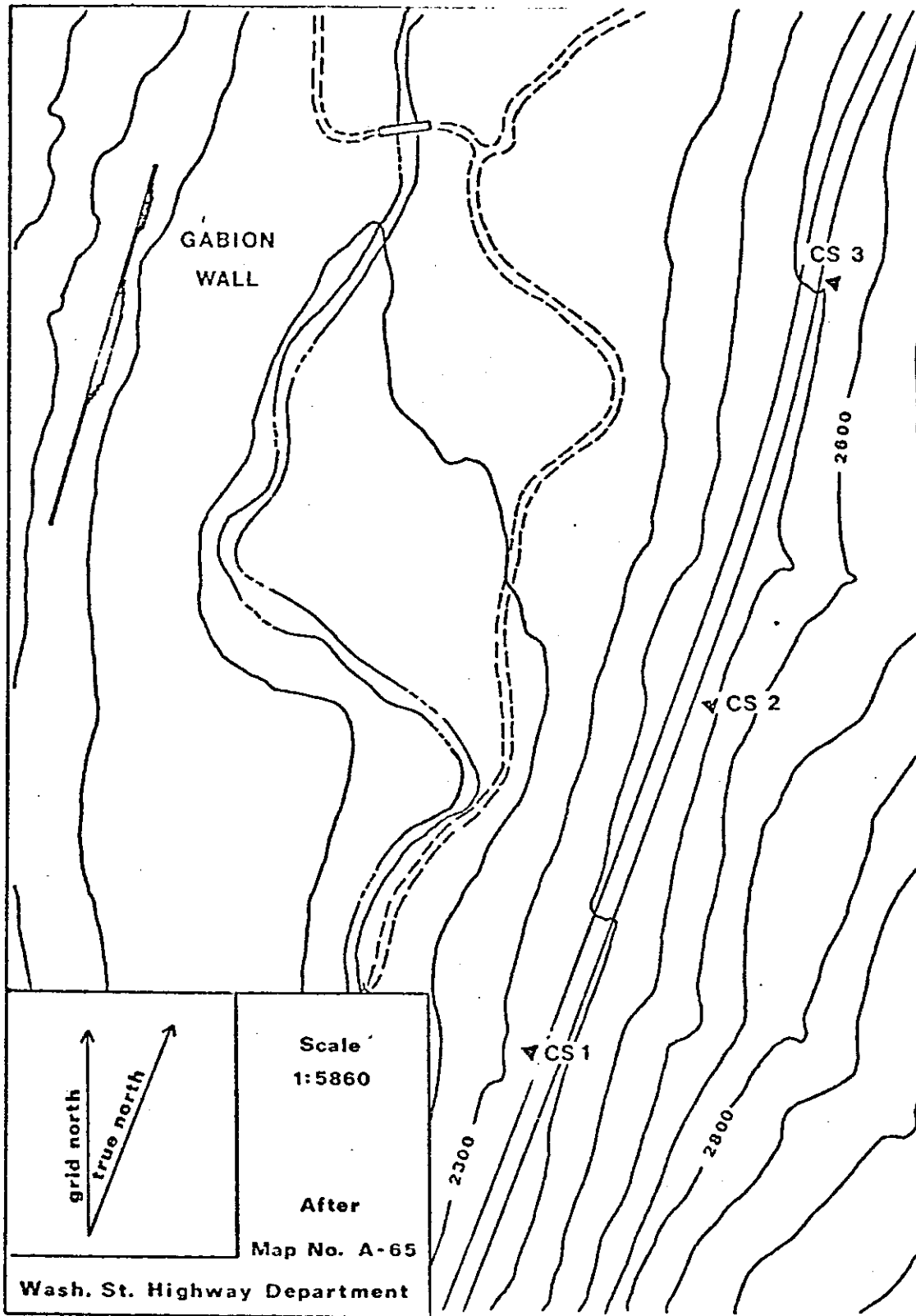


Figure 4

Area Topographic Map



ing movements are minimized.

In this section, two closely related camera mounts have been designed so as to incorporate convergent photography of 100 per cent overlap. This was accomplished by positioning the mounts at camera stations CS1 and CS3 permanently and having the third mount at camera station CS2 rotational, about an aft fixed vertical axis located on the camera axis itself.

The methodology applied to the construction of the three camera stations and the future attachment of the camera mounts to the stations is such that both behave as one integrated unit.

Camera stations CS1 and CS3 were anchored to bedrock by 3 cm x 3 cm reinforcement bars which were threaded on top to attach the camera mounts for each respective station. Camera station CS3 had additional 30 cm extensions welded to the bar ends so that the station could be elevated enough to clear the ground immediately in front of the camera station. Also, this served to allow the rods to be set deeper into the bedrock as the bedrock at this site is well jointed and highly fractured porphyritic basalt.

A drilling jig was prepared by the Washington State Highway Department's Soils Testing Laboratory at Tumwater to aid in aligning the holes so that the camera mounts at these two stations could be positioned and/or rotated about the rear collar to allow the desired photographic coverage. The jig was aligned so that its center line pointed to the center of the Gabion Wall. In this manner the mounts could be turned up to approximately 12° either left or right of center

if corrections had to be made in order to provide total wall coverage. One reason for this safeguard was that the wall's exact position, length and height were not known at the time of the establishment of the camera stations.

After the jig was aligned, using the three holes outlined by the triangle, holes were drilled deep enough to provide a level footing for the three legs. The reinforcement bars, which were bolted to a thin sheet of aluminum having the same hole dimension as the mounts for CS1 and CS3, were then placed in the drilled "pockets" and mortared in a level position.

When the mortar had set, the forming template was removed and forms measuring 56 cm in length and 53 cm in width were built around the three legs so as to form a level base up to the bottom of the threaded reinforcement bars for the camera mount to rest on. Hand mixed mortar was prepared at each camera station at a ratio of three sand to one cement. A small amount of coarse aggregate was hand-placed in each form to help add volume and mass to the camera pads. Water was obtained from nearby streams and was assumed to be of good quality. Ottawa sand was used as the fine aggregate and the cement was a composite mix of various types of cement from the Washington State Highway Department's Soils Testing Laboratory; and thus, the innate qualities or specifications of the cements are not known.

Camera station CS1 is located off the shoulder of the westbound lanes of Interstate 90 approximately 350 meters south of the viewpoint overlooking Denny Creek Campground and can be arrived at by taking Interstate 90 east to Snoqualmie Summit Recreation Area, exiting and

and turning back westbound onto Interstate 90.

Camera station CS3 can be found by driving east of the same viewpoint as described above approximately 550 meters, departing the auto and taking the alder overgrown grade along the toe of the exposed fault debris about 200 meters up to the camera station. Caution must be exercised in wet or freezing climate conditions due to the hazard of falling rock from above.

Camera station CS2 can be arrived at by taking Forest Service Trail Number Four to the second switchback and then proceeding approximately 200 paces south along the crest of the wooded bank across a stream to a granite outcrop which has an unobstructed view of the project area.

Camera station CS2 was unique in that it was the best situated so as to encompass the widest view of the opposite valley with the least amount of site preparation. It is constructed essentially in the same manner as camera station CS1 and CS3 except that four drilled and tapped reinforcement bars were used instead of three threaded bars. The drilling jig was used to make four holes, outlined by the rectangle and the camera was aligned so that it was set squarely to the approximate midsection of the Gabion Wall.

After the bars had been set, a form was built so that the mortar, which was hand-placed, would be level to within three or four millimeters with the top of the reinforcement bar. This was to allow room for the plaster of Paris to be placed between the rough concrete pad and the bottom plate of the camera mount. Figure 5 illustrates a cross-sectional view of camera station CS2 and how it was constructed.

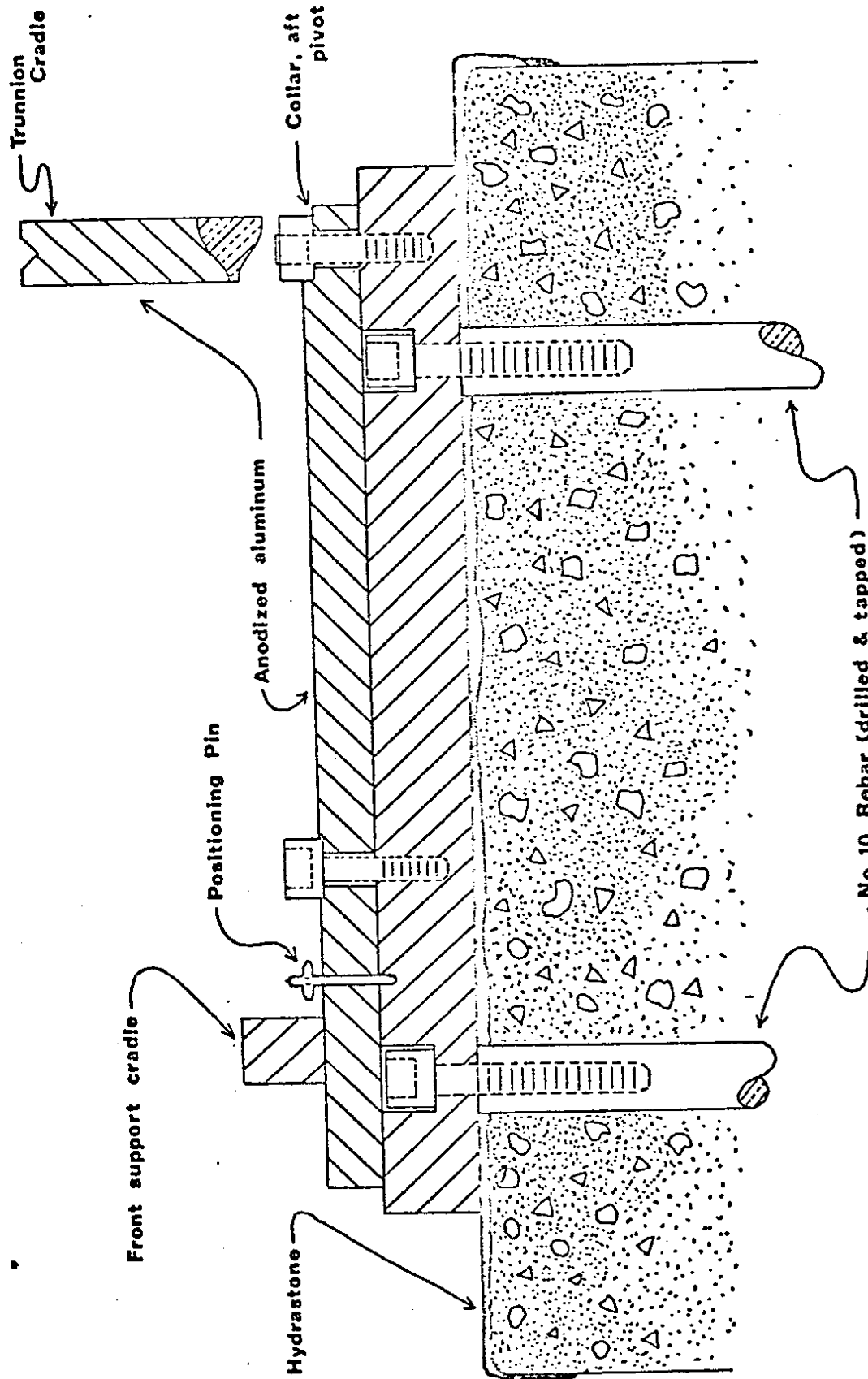


Figure 5  
Cross-Sectional View of Camera Station  
CS 2 and Mount  
(Not to Scale)

The reason for two plates at this station is that in order for the camera to produce correct and complete overlap of the Gabion Wall, the mount must be indexed at different locations.

### 3.2 Design of Targets

To measure the monitoring of the Gabion Wall using photogrammetric methods, the precise accuracy depends upon the pointing identification of the floating mark on the analytical plotter, (AP/C), or other instruments.

Maximum contrast between the target and its background is a primary consideration. Best results are obtained with a white target on a black background.

Experiments were carried out using a Galileo-Santoni terrestrial camera and different colored targets; red on white, blue on white, black on white, red on white and black on white. The results showed that white is the best color for the target material. Dark-colored earth or rocks of the Gabion Wall provide an excellent background.

Pointing on a circular target can reach extremely high precision for targets with small annuli. (August 1973 ASP)

However, circular targets in highly convergent photography become elliptical in shape due to the tilting of the photographs.

On the negative the measuring mark on the stereoplotter is pointed on a white circle of designated size. The size of the circle on the photograph should be larger than the 0.040 mm floating mark. The maximum accuracy is obtained when a smaller black measuring mark is centered on a larger white circular target.

Using a KA-2 modified terrestrial camera, tests were conducted

from the minimum photographable distance ( $h$ ) of 370 m (about 1200 ft.). After taking the photograph, the plate was developed and the resulting images were examined on the AP/C plotter. The best measurement was found to be obtained when the targets were 70 microns in diameter with a measuring dot of 40 microns.

The topographical map in Figure 4 shows the proposed Gabion Wall and the three camera stations.

Measurement of the angles was accomplished by the use of a protractor while distances were read from an engineer's scale.

Due to the tilt of the photograph, the circular target will exhibit two diameters (see Figure 6),  $D$  and  $D'$  in opposite directions.  $D$  is equal to the minor axis of the ellipse in which the diameter represents a function of the parallax angle ( $\beta$ ), focal length, floating mark ( $d$ ), and perspective angle ( $\alpha$ ).

The following formula for convergent photography is

$$D = D'_{\min} \frac{\sin(\alpha + \beta)}{\sin \alpha} \dots \dots \dots (1)$$

$$D'_{\min} = d (h/f) \dots \dots \dots (2)$$

$$D'_{\max} = \frac{7d}{5f \sin \alpha} h_i \dots \dots \dots (3)$$

where  $h_i$  is the vertical distance between the Gabion Wall and a particular camera station.

Measurement from Camera Station 1:

Perspective angle ( $\alpha$ ) = 29.5 degrees

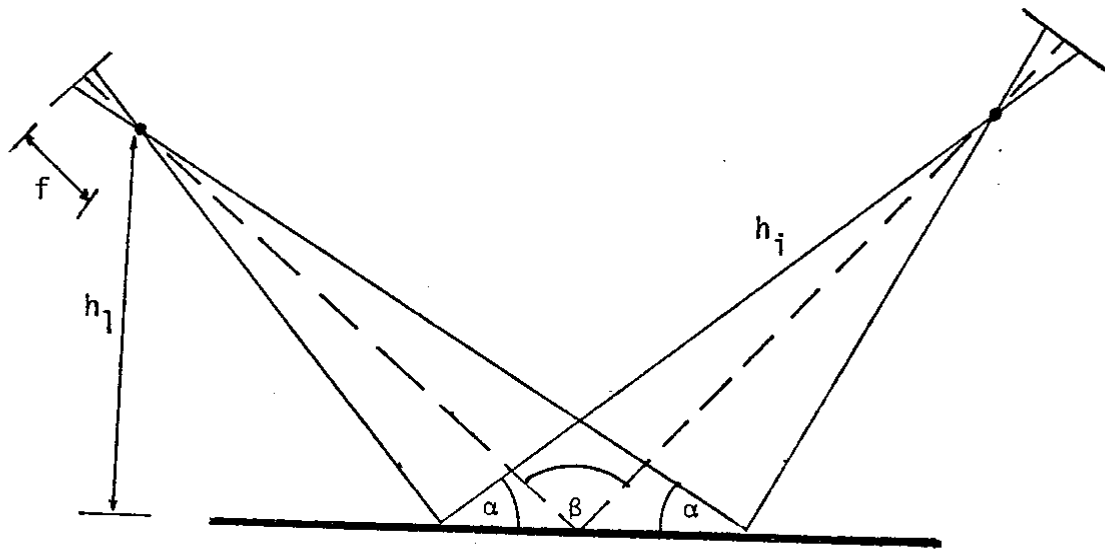


Figure 6  
Convergent Photography

Parallatic angle ( $\beta$ ) = 55.5 degrees

$h_i$  = 900 m (the distance between camera and critical target)

$h_1$  = 440 m

$d$  = 40 micron (diameter of measuring mark)

$f$  = 615 mm (focal length)

$D_{\min}$  = 12.02 cm       $D_{\max}$  = 16.55 cm (computed from equations (2) and (3))

Measurement from Camera Station 2:

Perspective angle ( $\alpha$ ) = 77 degrees

Parallatic angle ( $\beta$ ) = 55.5 degrees

$h_i$  = 720 m

$h_1$  = 590 m

$D_{\min}$  = 3.57 cm       $D_{\max}$  = 4.18 cm

From the computational result, the minimum diameter of the target is 12 cm which was computed from Camera Station 1. The targets photographed from Camera Station 2 were computed to have a minimum diameter of 3.57 cm.

To insure use of the targets for every camera station, a target with a diameter between 12 cm and 16 cm must be used.

The photographic properties of plates type IV-F relate to their ability to produce a satisfactory record through the actions of exposure and processing. Different physical characteristics of photographic processing affect their photographic properties. The preliminary test plates were developed by the University of Washington's Photographic Division at the Audio Visual Center. Due to the fact that the development of these plates is critical in terms of proper



exposure, the later development and processing of these plates was done by the Photogrammetric Division at the Washington State Highway Department. The plates developed by the Highway Department were found to be of a better quality, measurable in terms of target to background contrast.

### 3.3 Base Line and Control Net Measurement and Adjustment

The control net which determines the position of camera stations was established along the existing Interstate 90 (to be east bound when completed). This is a very narrow piece of land on which to establish a network of desirable geometry. The topographic map of the area is shown by Figure 4. Thus it resulted in a network with ill conditioned geometry. This situation required a combination of angle and distance measurement to arrive at an accuracy which is required for such a project.

The geometry is exhibited in Figure 7 where the measured angles are noted as 1 to 8. The smallest angle is 56 minutes. Because of the ill conditioned geometry, a sequential adjustment was used in order to eliminate values having an adverse influence on the accuracy.

The sequences of adjustments were:

1. Adjustment of Base Lines (Points 1, 1a and 3)
2. Determining the Position of Point 2a.
3. Adjustment of Camera Station 2

(in Figure 7 CS 1, CS 2 and CS 3 were used as Camera Stations)

For the adjustment of base lines, two sets of electronic surveying measurements were used. One was measured in the fall of 1975 by Tellurometer DC-6 and the second set was measured in the spring of

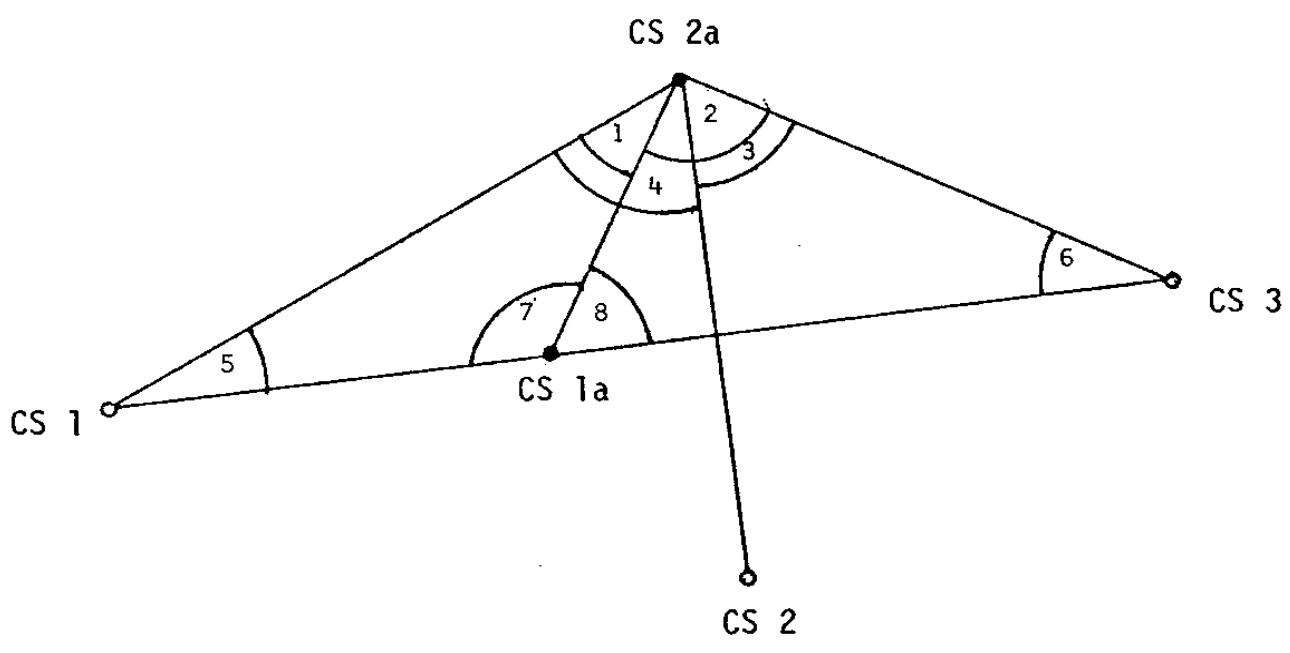


Figure 7  
Adjustment of Camera Stations

1976 by Kern DM 500. The results of these measurements are shown in Table 1. From the Table it was concluded that there was no motion of points during the winter in spite of the geological faults which are close-by.

Table 1  
Comparison of Base Line Measurements

Station	<sup>CD-6</sup> Tellurometer	Kern DM 500
CS 1-CS 3	736.919 m	736.9005 m
CS 1-CS 1a	105.495 m	105.5217 m
CS 3-CS 1a	631.421 m	631.3828 m
CS 2a-CS 2	52.742 m	52.7395 m

The adjustment of the base line was done by the observation method with the observation equation in general form of:

$$AX - L = V$$

and the most probable values are:

$$CS 1 - CS 1a = 105.5204 \text{ m} \pm 1.9 \times 10^{-3} \text{ m}$$

$$CS 1a - CS 3 = 631.3815 \text{ m} \pm 1.9 \times 10^{-3} \text{ m}$$

$$CS 1 - CS 3 = 736.9010 \text{ m} \pm 1.9 \times 10^{-3} \text{ m}$$

A combined intersection and resection method of adjustment were used to determine the position of point CS 2a using 5, 6, 8 and 1 and 2 angles respectively. The method of observation with quasi-normal was used in adjustment in which the basic formulas are:

$$\begin{bmatrix} AX - L = V \\ DX - J = V' \end{bmatrix}$$

and the normal equation matrix is:

$$[A^T P A, D^T P' D] X - [A^T P L + D^T J] = 0$$

For a detailed solution of these equations, the reader is referred to Veress, 1974 reference. This adjustment resulted in the most probable values of coordinates of point CS 2a with the standard errors of:

$$\sigma_x = \pm 7.5 \times 10^{-3} \text{ m}$$

$$\sigma_y = \pm 2.3 \times 10^{-3} \text{ m}$$

Finally, the position of CS 2 station was determined with the least-squares adjustment of observation method resulting in a standard error of coordinates being less than 2 mm. The elevation of these points were determined by trigonometric leveling adjusted by least-squares. The standard errors were found to be between  $\pm 0.006$  and  $0.003$  m.

#### 4.0 FUNDAMENTAL PHOTOGRAMMETRIC QUANTITIES FOR MONITORING

The character of this chapter will deal with essentially two major points. The first includes the method of determination of the ground coordinates of the frontal nodal points  $X_{1f}$ ,  $Y_{1f}$ ,  $Z_{1f}$ ,  $X_{2nf}$ ,  $Y_{2nf}$ ,  $Z_{2nf}$ ,  $X_{2sf}$ ,  $Y_{2sf}$ ,  $Z_{2sf}$ , and  $X_{3f}$ ,  $Y_{3f}$ ,  $Z_{3f}$ . Secondly, a precise method must be developed to obtain four separate orientation matrices for the four camera positions used during the monitoring procedure. With these matrices, a Sign Convention must be established which could be systematically applied in this project.

#### 4.1 Coordinates of Frontal Nodal Points

A camera pedestal has been permanently fixed at each of the Camera Stations to ensure consistency in the orientation of the camera during monitoring. It enables the user to occupy the Station at any

time without the need to re-determine Orientation Parameters. In order for the camera to be independent of the existing field control, it is necessary to determine the coordinates of the frontal nodal points. The camera is suspended on an aluminum pedestal which is fixed to the Camera Station. The following procedure describes the method of coordinate determination of the frontal nodal point. As illustrated by Figure 8, the control point (1c), located approximately 2 meters from CS 1, was constructed so that it lies on the base line formed by CS 1 and CS 3. A T-2 theodolite was set up at point 1c (see Figure 9) and angles were observed between 1b and 1f which represent the frontal nodal point and vertical center of the camera place respectively. Distances were measured using a steel tape. To ensure an accuracy of 0.5 mm, the distance was measured between these points 10 times. Thus, the coordinate of 1f is obtained by following formulas and numerical expressions:

$$\begin{aligned} X_{1f} &= X_{1c} - d_1 \cos \phi_1 = 1000.1702 \text{ meters} \\ Y_{1f} &= Y_{1c} - d_2 \cos \phi_2 = 1000.0738 \text{ meters} \\ Z_{1f} &= Z_{cf} + \Delta Z = 1000.222 \text{ meters} \dots \dots \dots (4) \end{aligned}$$

where  $Z_{1f}$  is computed from the known CS 1 elevation,  $\Delta Z$  being the measure between CS 1 and the camera principal line.

Similarly the coordinates of 3f at Camera Station 3 (CS 3) can be obtained:

$$\begin{aligned} X_{3f} &= X_{3c} + d_1 \cos \phi_1 = 1736.467 \text{ meters} \\ Y_{3f} &= Y_{3c} + d_1 \cos \phi_1 = 1000.139 \text{ meters} \\ Z_{3f} &= Z_{3c} + \Delta Z = 1055.26 \text{ meters} \dots \dots \dots (5) \end{aligned}$$

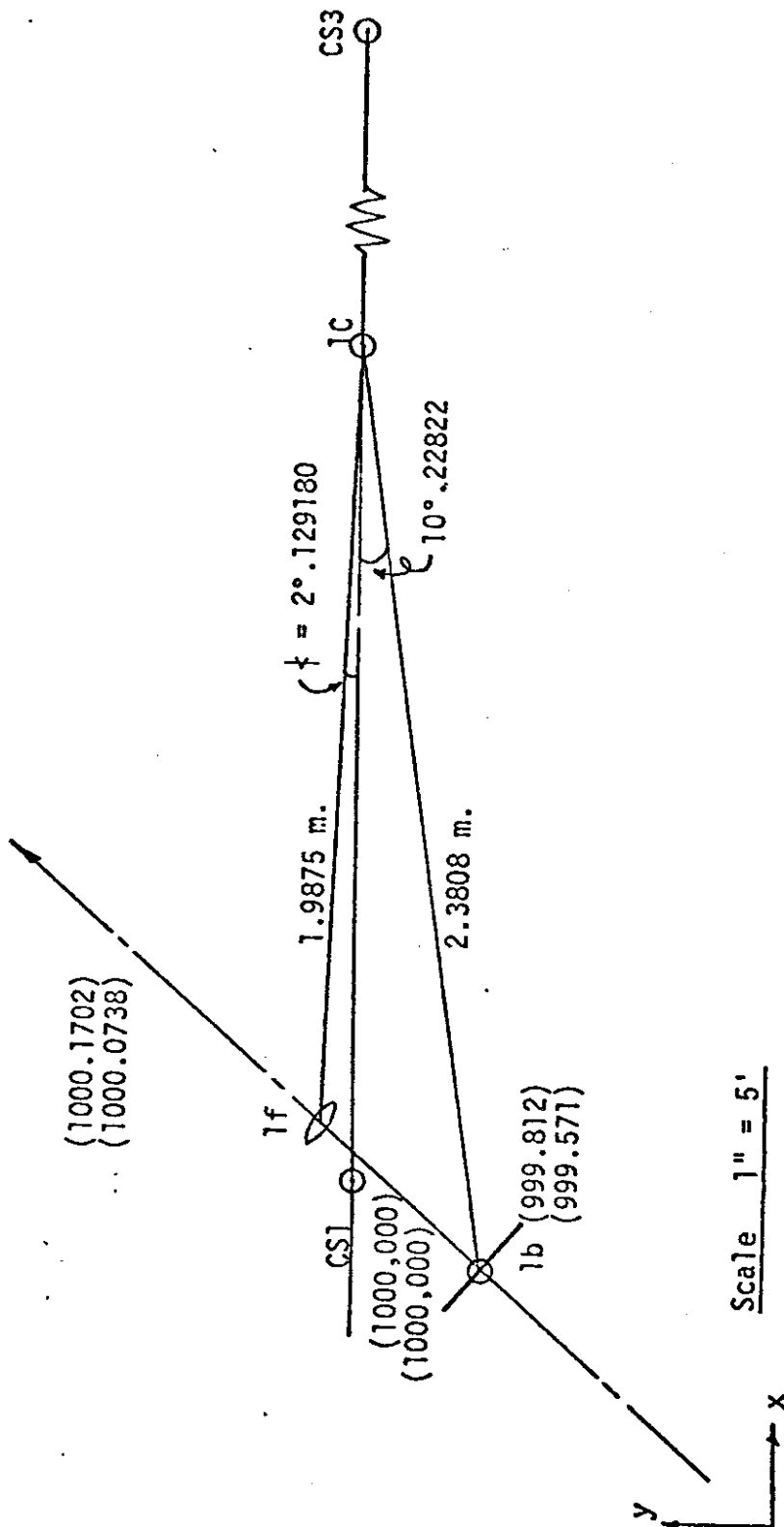


Figure 8  
Coordinate of Frontal Nodal Point at Camera Station One

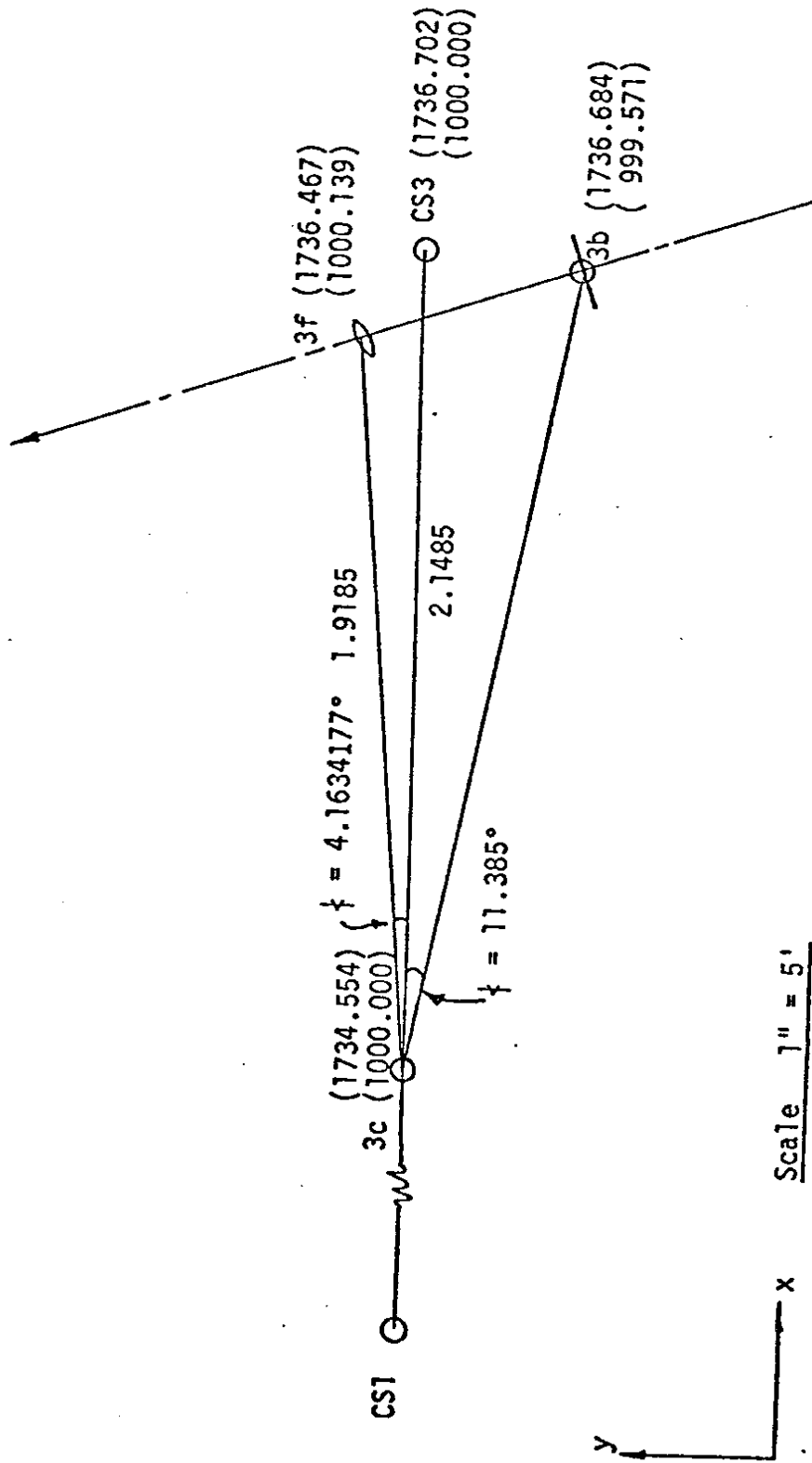


Figure 9  
Coordinate of Frontal Nodal Point at Camera Station Three

The geometric sketch is shown in Figure 9.

At Camera Station 2, the point 2c was established on the bedrock near CS 2 on line with Camera Station CS 2 and control point CS 2a. Since Camera Station CS 2 is allowed to rotate, two frontal nodal points at this station must be determined. The following shows the mathematical expressions used in the computation.

The southern most frontal nodal point,  $3_{sf}$ , can be obtained by

$$\begin{aligned} X_{2sf} &= X_{2c} + d_1 \sin (\text{Azimuth} - \dagger 1) = 1376.897 \text{ meters} \\ Y_{2sf} &= Y_{2c} + d_1 \cos (\text{Azimuth} - \dagger 1) = 963.607 \text{ meters} \\ Z_{2sd} &= Z_{CS2} + \Delta Z = 1048.428 \text{ meters} \dots \dots \dots (6) \end{aligned}$$

Here, the Azimuth computed relies on CS 2a and CS 2 where  $\Delta Z$  is directly measured by tape.

The northern most frontal nodal point,  $2_{nf}$ , can be obtained by

$$\begin{aligned} X_{2nf} &= X_{2c} + d_2 \sin (\text{Azimuth} - \dagger 2) = 1376.965 \text{ meters} \\ Y_{2nf} &= Y_{2c} + d_2 \cos (\text{Azimuth} - \dagger 2) = 963.849 \text{ meters} \\ Z_{2nf} &= Z_{CS2} + \Delta Z = 1048.428 \text{ meters} \dots \dots \dots (7) \end{aligned}$$

The other control points,  $1_b$ ,  $2_{sb}$ ,  $2_{nb}$  and  $3_b$  are derived as in the previous computation. Table 2 summarizes the coordinates of all camera station points with the approximate  $\omega$  camera orientation given for future comparisons. All these control points,  $3_c$ ,  $2_c$  and  $1_c$  are monumented for further use or recalibration as may be required after the spring of 1976/77.

#### 4.2 Orientation of Camera Stations

The Camera Orientation Parameter ( $\omega$ ,  $\phi$ ,  $\kappa$ ) could be obtained by indirectly measuring distances and angles. The principle line of the KA-2 Camera is uncertain because it cannot be physically measured.



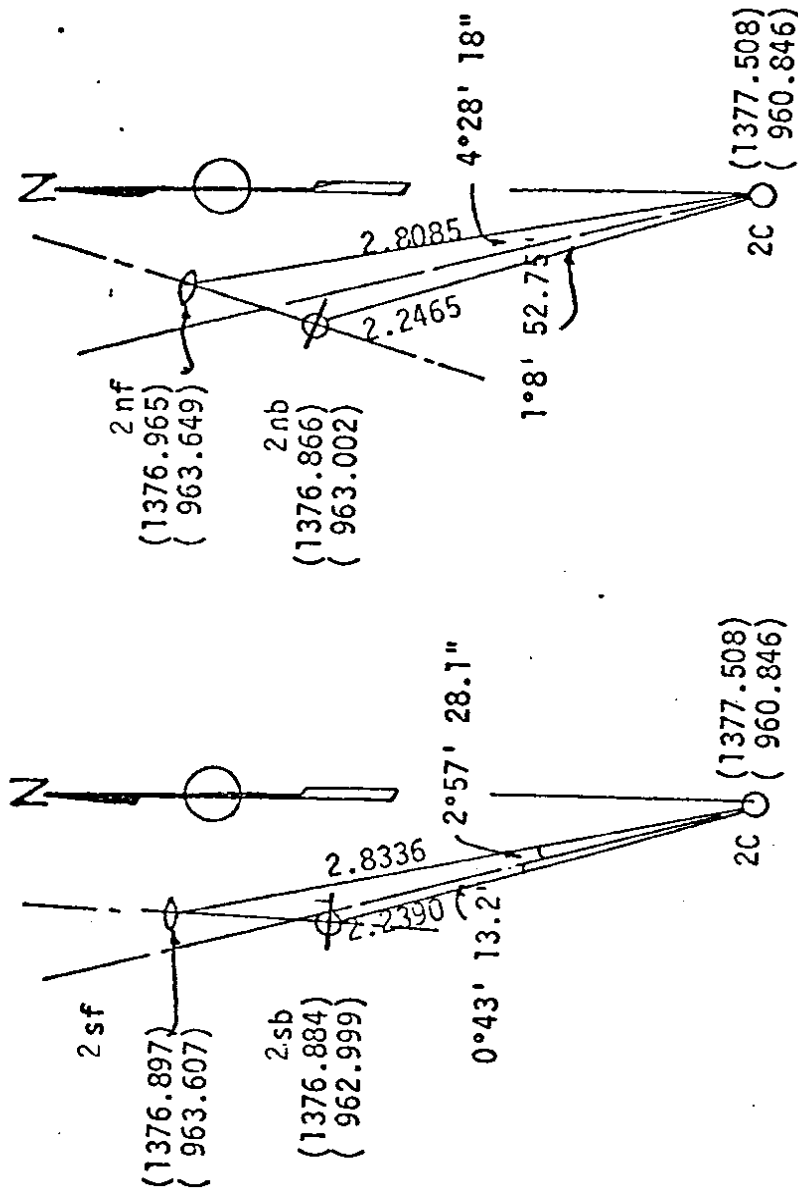
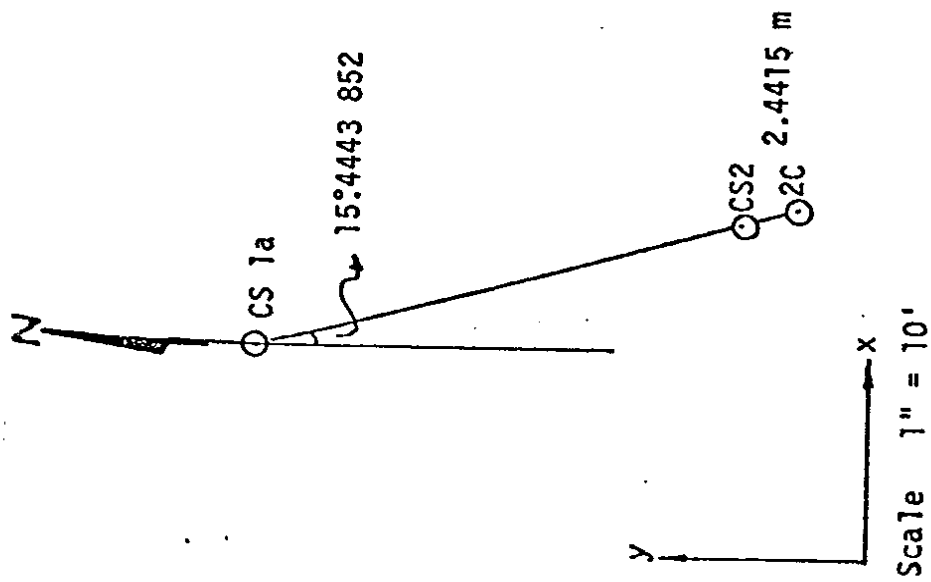


Figure 10  
Coordinates of Frontal Nodal Point at Camera Station Two

Table 2  
The Relation of Camera Station Coordinates with Frontal Points

Station	Point	Coordinate		$\omega = \tan \frac{\Delta X}{\Delta Y}$
		X	Y	
CS1	1f	1000.1702	1000.0738	35°79215003
	1b	999.812	999.577	
CS2	2sf	1376.897	960.607	1°224887594
	2sb	1376.884	962.999	
	2nf	1376.965	963.649	
	2nb	1376.886	963.002	
CS3	3f	1376.467	1000.139	8°699514927
	3b	1376.685	999.571	
				-20°99694286

From the previous computation, the  $\omega$  angle of the camera is not accurate enough. Indirect physical measurement of  $\omega$  has proven inadequate for monitoring over long distances. For long distances a striding level with the accuracy of 2 seconds of arc could be used for physically determining the  $\omega$  angle. This precise level was not available. Therefore, using control target to determine the orientation matrix is the only reliable method. Three known control points are needed to determine the orientation matrix of the camera. The following describes the determination of each of the Camera Stations.

Let the coordinates of point 0 be the frontal nodal point. The control point, P, is represented by the coordinates  $x_p$ ,  $y_p$ , and  $z_p$ . The vector,  $\vec{S}_p$ , is representative of the ray from the P image point to the photographic station. The vector,  $\vec{A}_p$ , is the ray from the control point to the image point. The image points can be measured under the AP/C. The focal length (f) is a calibrated value determined by U.S.G.S.

The components of  $S_p$  are:

$$\vec{S}_p = (-x_p, -y_p, f)$$

The unit vector can be shown by:

$$\vec{S}_p^o = \left( \frac{-x_p}{d}, \frac{-y_p}{d}, \frac{f}{d} \right) \dots \dots \dots (8)$$

where

$$d = \sqrt{x_p^2 + y_p^2 + f^2}$$

$$\vec{S}_p^o = (\cos XPO, \cos YPO, \cos ZPO)$$

The components of A are:

$$\vec{A}_p = (Z_o - Z_p), (Y_o - Y_p), (Z_o - Z_p)$$

The Unit could be shown as:

$$\vec{A}_p^o = \left( \frac{X_o - X_p}{op}, \left( \frac{Y_o - Y_p}{op} \right), \left( \frac{Z_o - Z_p}{op} \right) \dots \dots \dots (9)$$

The relationship between the  $\vec{A}_p^o$  and  $\vec{S}_p^o$  is:

$$M \vec{S}_p^o = \vec{A}_p^o \dots \dots \dots (10)$$

The M orientation matrix has nine terms, consequently, three control points are required to determine the components. Let these points be P<sub>1</sub>, P<sub>2</sub> and P<sub>3</sub>. Then:

$$M (\vec{S}_{P_1}^o, \vec{S}_{P_2}^o, \vec{S}_{P_3}^o) = (\vec{A}_{P_1}^o, \vec{A}_{P_2}^o, \vec{A}_{P_3}^o)$$

where M in detail represents the following matrix:

$$\begin{matrix} \cos\phi\cos\kappa, & \cos\omega\sin\kappa + \sin\omega\sin\phi\cos\kappa, & \sin\omega\sin\kappa - \cos\omega\sin\phi\cos\kappa \\ -\cos\phi\sin\kappa, & \cos\omega\cos\kappa - \sin\omega\sin\phi\sin\kappa, & \sin\omega\cos\kappa + \cos\omega\sin\phi\sin\kappa \\ \sin\phi, & -\sin\omega\cos\phi, & \cos\omega\cos\phi \end{matrix}$$

The orientation matrix of Camera Station One is determined by four control points and found to be:

.8105467567	-.0073971802	-.5844774898
-.0066878548	.9971907512	-.0102709216
.5849800678	.0114596451	.8109903021

The Orientation Matrix of Camera Station CS 2S is determined by three control points:

1.0031849644	-.0179422285	-.0208884538
.0096826026	1.0009728530	.0245590382
.0194819124	-.0277419714	.9994585153

The Orientation Matrix of Camera Station CS 2N is determined by three control points:

.9336571101	-.0057673192	.3578149140
-.0111658707	.9977095075	.0314666542
-.3578752164	-.0338383871	.9331533254

#### 4.3 Data Collection

Due to the weight (120 lbs.) of the camera and the large elevation difference of the camera stations over which it has to be carried, a special backpack was modified to safely expedite its transport to the Camera Stations. A power source of 28 V.D.C. 14 AMP was obtained for the purpose of triggering the shutter. The power supply requirements were fulfilled by one 28 volt nickel-cadmium battery. Theoretically, the battery is operable for one month without requiring a recharge or the equivalent of taking at least 20 pictures.

One of the most important monitoring requirements is that the camera setting must have the same orientation during picture taking.

The KA-2 Camera is equipped with two heavy aluminum bands encircling the body of the camera. The larger cylindrical bars protrude on either side of the aft ring. This is designed to fix and give support to the camera on the camera pedestal. A knurled knob on the right side of the camera on the cylindrical bar holds the camera flush with the edge of the aluminum pedestal. On the front band is an aluminum foot which can be latched securely to the front retaining receptacle. These three points are needed to fix the orientation of the camera in space.

Unfortunately, this mechanical positioning does not firmly establish one set of orientation parameters. Temperature changes and imperfections in mechanical positioning induce a change in the orientation of the camera, thereby changing the values computed in the orientation matrices. The major problem involves play in the camera positions when seated on the pedestal at its three contact points. This problem originated partially from the construction of the front support of the camera. It was modified by a circular metallic piece which was added within the receptical and held in place with epoxy glue. This solution stabilized the camera to a desirable level.

The exposure of the photographs was determined by light meter measurement. The erratic nature of the atmosphere at Snoqualmie necessitates frequent light meter readings and aperture adjustments to obtain the proper exposure. The light meter must be positioned along the line of sight of the camera. Setting the ASA 50, the proper aperture and shutter speed were recorded. Since only a few shutter speeds are available, the aperture can be adjusted to obtain the proper exposure. Under the extremely foggy or rainy conditions, the monitoring should be cancelled because the obtained image appears out of focus, thus, technically not usable to obtain a high degree of accuracy. Experience dictates monitoring between 11:00 a.m. and 1:00 p.m. during sunlit periods and clear atmospheric conditions.

The photographs were developed by the Washington State Highway Department, Photogrammetric Laboratory. They provided negatives of excellent quality and uniform density.

#### 4.4 Data Reduction

The photographic coordinates of the negatives were obtained on the Analytical Plotter (AP/C) at the University of Washington. The accuracy of the photo coordinates were  $\pm 2 - 6$  microns. These results were obtained by five observations depending on the ambiguity of the targets. It was found that the increase in accuracy over two observations was seldom economically justifiable.

The photo coordinates as obtained by the AP/C were reduced to the center of the negatives by using two dimensional affine transformation. This is expressed mathematically as:

$$\begin{aligned}\bar{x} &= a_{11} x + a_{12} y + c_1 \\ \bar{y} &= a_{21} x + a_{22} y + c_2 \dots \dots \dots 11\end{aligned}$$

Then using the orientation matrix, a space intersection was performed to determine the spatial coordinates of targeted points. The space intersection can be briefly described from camera station  $i$  and  $j$  as follows. The vectors from the camera stations to the object points are designated as:

$$\begin{aligned}\vec{S}_I &= (\cos XPO_i, \cos YPO_i, \cos ZPO_i) \\ \vec{S}_J &= (\cos XPO_j, \cos YPO_j, \cos ZPO_j)\end{aligned}$$

The relation between the vectors of picture and object space are:

$$M_i \vec{S}_i = \vec{S}_I \text{ and } M_j \vec{S}_j = \vec{S}_J \dots \dots \dots 12$$

The equations of line  $O_iP$  and  $O_jP$  are:

$$\begin{aligned}\frac{X_P - X_{O_i}}{\cos XPO_i} &= \frac{Y_P - X_{O_i}}{\cos YPO_i} = \frac{Z_P - Z_{O_i}}{\cos ZPO_i} \\ \frac{X_P - X_{O_j}}{\cos XPO_j} &= \frac{Y_P - Y_{O_j}}{\cos YPO_j} = \frac{Z_P - Z_{O_j}}{\cos ZPO_j} \dots \dots \dots 13\end{aligned}$$

Using equations (12), the direction cosines are computed and the  $X_p$ ,  $Y_p$ , and  $Z_p$  of the target point coordinates are obtained from equation (13) by means of least-squares adjustment.

The above described procedure is used for routine procedure. In this case, however, due to the fact that the purpose of this project is research in addition to the routine data production, space resection and computation of orientation matrices were also performed. These data were used to analyze the results to be discussed in the following chapter in detail.

This space resection and the computation of the orientation matrices were based on control points. These points were permanently mounted on the mountainside in bedrock. Their positions were determined by angulation from the base lines (CS 1, CS 3) using Kern DKM-3 theodolite.

The list and nature of the monitored points are given in Table 3. The identification of these points were taken from a 24"x36" enlargement which has been transferred to the Washington State Highway Department and is, therefore, omitted from here.

## 5.0 RESULTS AND ANALYSIS

### 5.1 Data Output

As shown by Table 3, there were three different types of points observed during the monitoring process. They were control points, targeted points and natural points or targets. The control points are coded as 800's and 900's while the other points are continuously numbered from 1 on.



TABLE 3 LIST OF PHOTOGRAMMETRICALLY MONITORED POINTS

1977

1976

TYPE OF POINT	SEP 07	OCT 12	OCT 18	OCT 27	NOV 03	NOV 23	DEC 01	JAN 28	APR 12	MAY 26
CONTROL	991	991	991	991	991	991	991	991	992	991
	992	992	992	992	992	992	992	992	992	992
	993	993	993	993	993	993	993	993	993	993
	994	994	994	994	994	994	994	994	994	994
	---	881	---	881	881	881	---	---	---	---
	---	882	882	882	---	---	882	882	882	882
	---	883	883	883	883	---	883	883	883	883
	---	884	884	884	884	884	884	884	884	884
	---	---	886	886	886	886	886	---	886	886
ARTIFICIAL TARGETS	---	---	---	005	005	005	005	---	005	---
	006	006	006	006	---	006	006	---	006	---
	008	008	008	008	---	008	008	---	008	---
	009	009	009	009	---	---	---	---	---	---
	010	010	010	010	010	010	010	010	010	010
	011	011	011	011	011	011	---	---	---	---
	012	012	012	012	012	012	---	---	---	---
	013	013	013	013	013	---	---	---	---	---
	016	016	016	016	016	016	016	016	016	016
	018	018	018	018	018	018	018	018	018	018
	041	041	041	041	041	041	041	041	041	041
	042	042	042	042	042	042	042	042	042	042
	043	043	043	043	043	043	043	043	043	043
	044	044	044	044	044	044	044	044	044	044
	060	060	060	060	060	060	060	---	060	060
	---	---	---	---	---	061	---	---	061	---
	067	067	067	067	067	067	067	067	067	067
	---	084	084	084	084	084	---	---	084	084
	---	086	086	086	---	---	---	---	086	086

TABLE 3 Continued:

TYPE OF POINT	1976					1977				
	SEP 07	OCT 12	OCT 18	OCT 27	NOV 03	NOV 23	DEC 01	JAN 28	APR 12	MAY 26
ARTIFI- CIAL TARGETS, CONT.	---	088	088	088	088	088	---	---	088	088
	097	097	097	097	097	097	---	---	097	097
	---	---	101	101	101	101	101	101	101	101
	---	---	102	102	102	102	102	102	102	102
	113	113	113	113	113	---	---	---	---	---
	---	---	201	201	201	201	201	201	201	201
	---	---	203	203	203	203	203	203	203	203
	---	225	225	225	225	225	225	---	---	---
	---	302	302	302	302	302	302	---	---	---
	---	303	303	303	303	303	303	---	---	---
	---	304	304	304	304	304	304	---	---	---
	---	305	305	305	305	---	---	---	---	---
	---	402	402	402	402	402	402	---	---	---
---	523	523	523	523	523	523	---	---	523	
NATURAL TARGETS	151	151	151	151	---	---	---	---	---	---
	152	152	152	152	---	---	---	---	---	---
	153	153	153	153	---	---	---	---	---	---
	154	154	154	---	---	---	---	---	---	---
	155	155	155	---	---	---	---	---	---	---
	161	161	161	---	---	---	---	---	---	---
	162	162	162	---	---	---	---	---	---	---
	163	163	163	---	---	---	---	---	---	---
	164	164	164	---	---	---	---	---	---	---
	165	165	165	---	---	---	---	---	---	---
	166	166	166	---	---	---	---	---	---	---
	171	171	171	---	---	---	---	---	---	---
	172	172	172	---	---	---	---	---	---	---
	173	173	173	---	---	---	---	---	---	---
	174	174	174	---	---	---	---	---	---	---
	175	175	175	---	---	---	---	---	---	---
	176	176	176	---	---	---	---	---	---	---
	---	177	177	---	---	---	---	---	---	---
185	185	185	185	185	185	185	---	---	185	

TABLE 3 Continued:

TYPE OF POINT	1976				1977					
	SEP 07	OCT 12	OCT 18	OCT 27	NOV 03	NOV 23	DEC 01	JAN 28	APR 12	MAY 26
	186	186	186	186	---	---	---	---	186	---
	187	187	187	187	---	---	187	---	187	187
	188	188	188	188	---	---	---	---	188	---
	189	189	189	189	---	---	---	---	---	---
	251	251	251	251	251	251	251	---	251	251
	252	252	252	252	252	252	252	---	252	252
	253	253	253	253	---	---	---	---	253	253
	258	258	258	258	258	258	258	---	258	258
	259	259	259	259	259	259	---	---	259	259
	260	260	260	260	---	---	---	---	260	260
	261	261	261	---	---	---	---	---	---	---
	271	271	271	271	271	271	271	---	271	271
	272	272	272	272	272	272	272	---	272	272
	273	273	273	273	---	---	273	---	273	273
	274	274	274	---	---	---	---	---	274	---
	351	---	351	---	---	---	---	---	351	---
	---	---	---	---	---	---	---	---	---	---
	---	371	371	371	371	---	364	---	371	---
	---	372	372	372	---	---	371	---	---	371
	---	373	373	373	373	---	---	---	---	---
	---	451	451	451	---	---	---	---	373	---
	---	452	452	452	---	---	451	---	451	---
	---	453	453	---	---	---	452	---	452	452
	---	461	461	461	---	---	---	---	453	---
	---	462	462	462	---	---	461	---	461	---
	---	463	463	463	---	---	462	---	462	---
	051	051	051	051	---	---	463	---	463	---
	052	052	052	---	---	---	---	---	---	---
	111	111	111	---	---	---	---	---	---	---
	116	116	116	---	---	---	---	---	---	---
	118	118	118	118	---	---	---	---	---	---
	---	226	226	226	---	---	---	---	---	---
	---	441	441	---	---	---	---	---	---	---
	444	444	444	---	---	---	---	---	---	---
	667	667	667	667	---	---	---	---	---	---

NATURAL  
TARGETS,  
CONT.

The position (X, Y, and Z) of all these points has been determined at each time photographs were taken. Along with these coordinates, the deviations from each coordinate from the "zero" data were also given. The "zero" data were considered to be the information from the first set of photographs which were taken on September 7, 1976.

A sample of the data output is given in Table 4.

A computer program has been used to tabulate the data continuously as the monitoring progressed. In the Table, the first two columns need no explanation. The third column gives the X coordinate of the points in meters and is printed out only to 1/100 of the meter but computed to 1/10,000 of the meter. The fourth column, DX, gives the deviation of the X coordinates from the "zero" data, that is, from September 7, 1976. For example, on January 28, 1977, the target was found to be 1.6 cm or 0.6 inches in a southerly direction from its September 7th position. (Note: this is a local coordinate system. See Figure 4 for the proper orientation.) This column is given in cm units. Columns 5, 6, 7 and 8 are in the same unit for Y and Z coordinates. The final column gives the number of camera stations or photographs from which the coordinates were determined. In Table 4, the number of photographs were consistently three but for some of the other points, the number of photographs were two or three. The accuracy of the results is dependent on the camera stations which necessitated this column as will be explained later in this chapter.

The analysis and the interpretation of the results can be done by numerical and graphical means. The numerical interpretation of the results can be done by tabulating the deviation of the coordinates

TABLE 4

## A SAMPLE OF THE DATA OUTPUT

DATE	POINT	X	DX	Y	DY	Z	DZ	NO. OF PHOTO-GRAPHS
Sept. 7	992	1429.65	.0	1029.32	.0	1647.73	.0	3
Oct. 12	992	1429.65	.0	1029.32	.0	1647.73	.0	3
Oct. 18	992	1429.65	.0	1029.32	.0	1647.73	.0	3
Oct. 27	992	1429.65	.0	1029.32	.0	1647.73	.0	3
Nov. 3	992	1429.65	.0	1029.32	.0	1647.73	.0	3
Nov. 23	992	1429.65	.0	1029.32	.0	1647.73	.0	3
Dec. 1	992	1429.66	-.2	1029.32	-.4	1647.73	-.5	3
Jan. 28	992	1429.64	1.6	1029.33	-.6	1647.71	1.9	3
Apr. 12	992	1429.66	-0.9	1029.33	-1.1	1647.71	2.3	3

in relation to the location of the points. For example, points 41, 42 and 43 are located in a nearly vertical line. In Table 5 the DZ coordinate deviations are given because they are the most important since they are perpendicular to the wall. The progressive motion of the wall can be seen from the table.

Graphical interpretation of the results are more illustrative. This is given in Figure 11. The figure well illustrates the deviation (in zig-zag form) of the "Mean Curve" (the continuous best fitting line). The zig-zag line indicates the variation of DZ due to the accuracy of the measurement. This problem will be discussed in detail in Section 5.3.

### 5.2 Stability of Orientation Matrices

The orientation matrix as derived from equation (10) can be shown as:

$$M = \begin{bmatrix} m_{11} & m_{12} & m_{13} \\ m_{21} & m_{22} & m_{23} \\ m_{31} & m_{32} & m_{33} \end{bmatrix}$$

where

$$m_{11} = \cos \phi \cos \kappa$$

$$m_{12} = \cos \omega \sin \kappa + \sin \phi \sin \omega \cos \kappa$$

$$m_{13} = \sin \omega \sin \kappa - \sin \phi \cos \omega \cos \kappa$$

$$m_{21} = -\sin \kappa \cos \phi$$

$$m_{22} = \cos \omega \cos \kappa - \sin \phi \sin \omega \sin \kappa$$

$$m_{23} = \sin \omega \cos \kappa + \sin \phi \cos \omega \sin \kappa$$

$$m_{31} = \sin \phi$$

$$m_{32} = -\sin \omega \cos \phi$$

$$m_{33} = \cos \omega \cos \phi$$

TABLE 5  
 Deviations of the DZ Coordinate

DATE	POINT	DZ	POINT	DZ	NO. OF PHOTO-GRAPHS
Sept. 17	41	0.0	42	0.0	3
Oct. 12	41	3.0	42	2.2	3
Oct. 18	41	1.8	42	0.4	3
Oct. 27	41	3.0	42	1.9	3
Nov. 3	41	5.5	42	4.0	3
Nov. 23	41	5.0	42	2.9	3
Dec. 1	41	5.7	42	4.8	3
Jan. 28	41	3.1	42	0.9	2
Apr. 12	41	9.7	42	9.2	3
May 26	41	10.4	42	9.6	3
June 10	41		42		

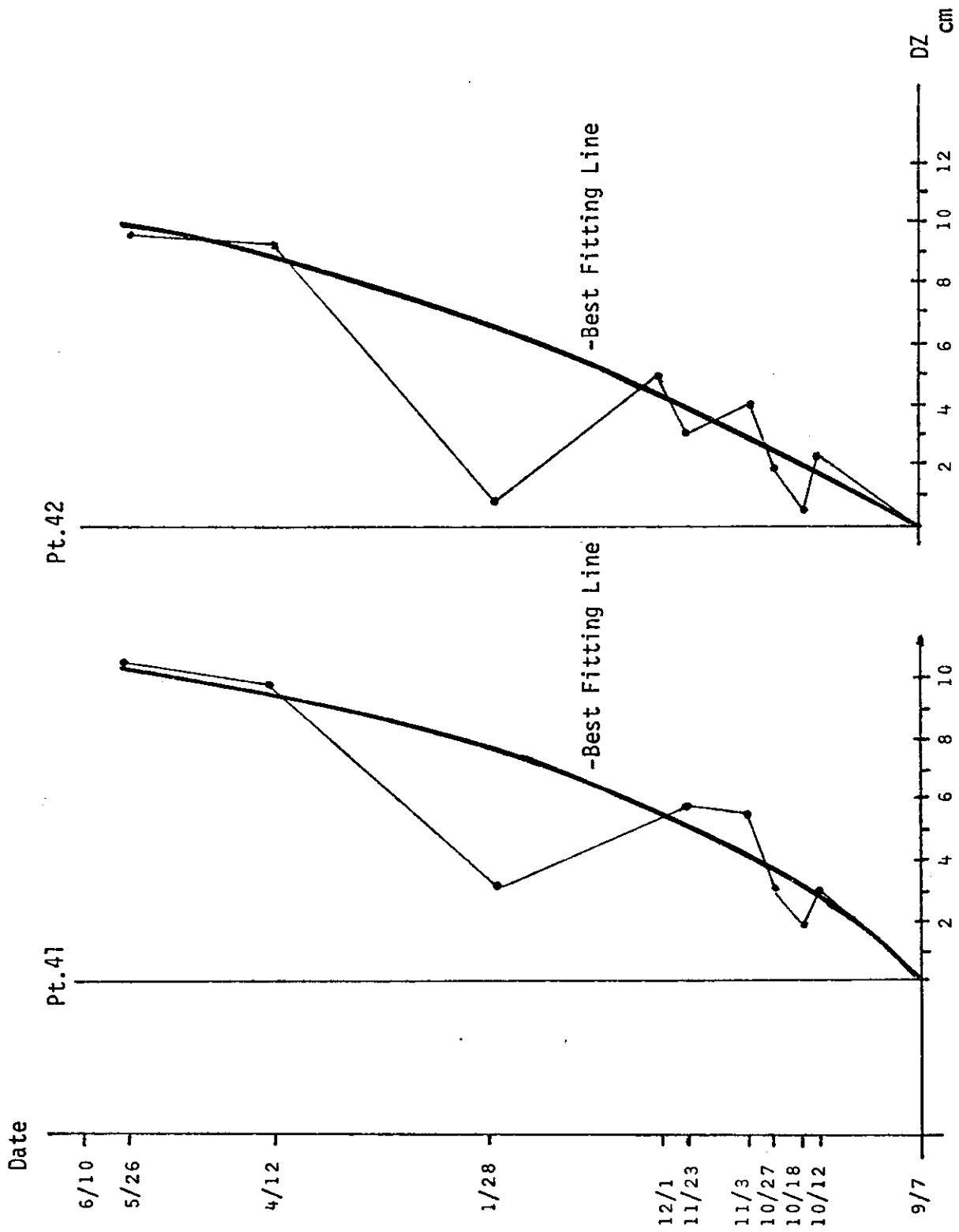


Figure 11

Deflection of Points 41 & 42



From these terms the rotational angles  $\phi$ ,  $\omega$ , and  $\kappa$  can be computed.  $\phi$  represents the rotation around Y or the vertical axis,  $\omega$  is the rotation around the X axis (parallel to the wall) and  $\kappa$  is the rotation around the Z or horizontal axis.

Thus

$$m_{31} = \sin \phi$$

Therefore

$$\phi = \sin^{-1} (m_{31}) \dots \dots \dots (14)$$

Further

$$\frac{m_{32}}{m_{33}} = - \tan \omega \dots \dots \dots (15)$$

The values of  $\omega$  can be determined after the appropriate change of sign has been made.

Also

$$\frac{m_{21}}{m_{11}} = - \tan \kappa \dots \dots \dots (16)$$

Thus, the values of  $\kappa$  can be determined similarly. Using equations (14), (15) and (16), the rotational angles  $\phi$ ,  $\omega$  and  $\kappa$  for the camera stations can be determined. The results are summarized in the following tables for Camera Stations CS 1 and CS 3. Camera Station CS 2 is used as a cross check and has less influence on the results. Thus it is omitted from here. The numerical results are given in Tables 6, 7, 8, 9, 10 and 11.

The  $\phi$  angle has the most influence on the coordinates of the point in the Z directions. Therefore, the variations of the  $\phi$  angle

TABLE 6

Variation of  $\phi$  angle at station CS 1

DATE			°	'	"
SEP	07	1976	35	50	16.130
OCT	12	1976	35	50	51.728
OCT	18	1976	35	50	20.3763
OCT	27	1976	35	50	21.9151
NOV	03	1976	35	50	22.0555
NOV	23	1976	35	47	50.2693
DEC	01	1976	35	50	22.0439
JAN	28	1977	35	50	42.6802
APR	12	1977	35	52	37.083
MAY	26	1977	35	50	25.2044

Mean =  $35^{\circ} 50' 24.9''$ 

TABLE 7

Variation of  $\omega$  angle at station CS 1

DATE			°	'	"
SEP	07	1976	-01	00	01.8083
OCT	12	1976	-01	02	35.7818
OCT	18	1976	-01	01	31.9973
OCT	27	1976	-01	01	39.4998
NOV	03	1976	-01	00	43.4225
NOV	23	1976	-00	43	43.5470
DEC	01	1976	-01	01	40.8609
JAN	28	1977	-00	50	19.3498
APR	12	1977	-00	45	35.4779
MAY	26	1977	-01	01	48.3967

Mean =  $0^{\circ} 56' 58.0''$

TABLE 8  
Variation of  $\kappa$  Angle at Station CS 1

DATE	°	'	"
SEP 07 1976	-00	34	4.2215
OCT 12 1976	-00	37	21.1902
OCT 18 1976	-00	32	27.9532
OCT 27 1976	-00	32	22.9950
NOV 03 1976	-00	32	23.4159
NOV 23 1976	-00	01	24.7327
DEC 01 1976	-00	32	21.4272
JAN 28 1977	-00	26	47.8627
APR 12 1977	-00	30	45.9273
MAY 26 1977	-00	32	35.6984

Mean  $\kappa = 0^{\circ} 29' 15.5''$

TABLE 9  
Variation of  $\phi$  Angle at Station CS 3

DATE	°	'	"
SEP 07 1976	-20	47	33.2172
OCT 12 1976	-20	47	31.1512
OCT 18 1976	-20	47	29.9484
OCT 27 1976	-20	47	28.1890
NOV 03 1976	-20	47	40.3981
NOV 23 1976	-20	47	31.1181
DEC 01 1976	-20	47	38.2747
JAN 28 1977	-20	45	11.1203
APR 12 1977	-20	47	41.5346
MAY 26 1977	-20	47	32.1941

Mean  $\phi = -20^{\circ} 47' 20.7''$

TABLE 10  
Variations of  $\omega$  Angle at Station CS 3

DATE			°	'	"
SEP	07	1976	01	54	51.2891
OCT	12	1976	01	53	44.6814
OCT	18	1976	01	53	39.4242
OCT	27	1976	01	53	41.7743
NOV	03	1976	01	53	33.3722
NOV	23	1976	01	53	43.1693
DEC	01	1976	01	53	31.2364
JAN	28	1977	01	--	--
APR	12	1977	01	56	24.7674
MAY	26	1977	01	53	44.6046

Mean  $\omega = 1^{\circ} 54' 06.0''$

TABLE 11  
Variations of  $\kappa$  Angle at Station CS 3

DATE			°	'	"
SEP	07	1976	-00	41	14.3165
OCT	12	1976	-00	38	03.1745
OCT	18	1976	-00	37	53.8778
OCT	27	1976	-00	38	20.6793
NOV	03	1976	-00	36	43.0093
NOV	23	1976	-00	37	59.3319
DEC	01	1976	-00	36	48.5777
JAN	28	1977	-00	--	--
APR	12	1977	-00	37	2.1907
MAY	26	1977	-00	38	30.0238

Mean  $\kappa = 0^{\circ} 38' 03.9''$

are also represented by graphical means for camera stations CS 1 and CS 3 in Figure 12.

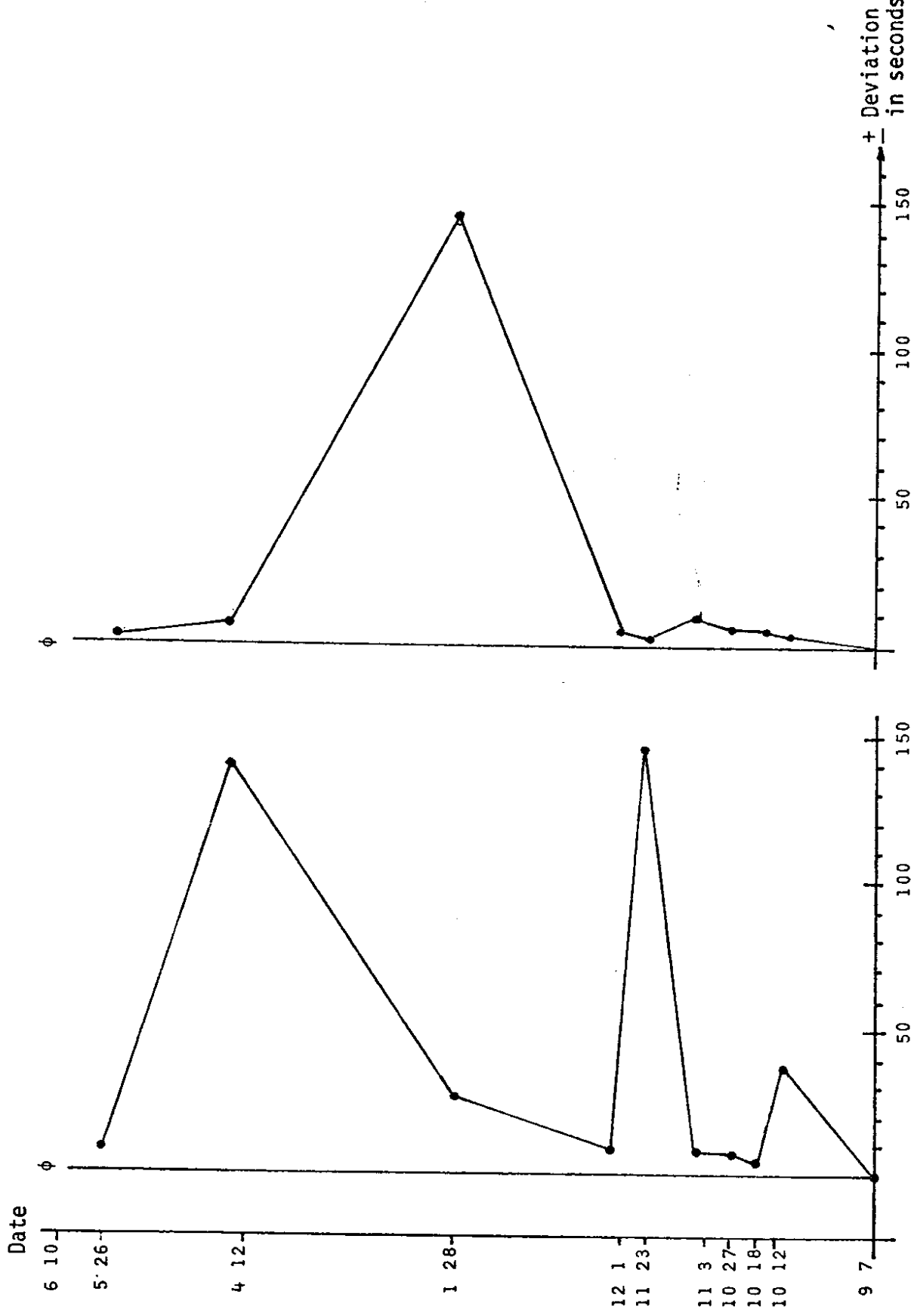
It can be seen from this Figure that the  $\phi$  angle is unstable at Camera Station CS 1. This is due to the fact that this station is located very close to the pavement of the westbound traffic of Temporary I-90 from which considerable vibration is transmitted to the camera by the vehicular motion. The maximum influence is in the  $\omega$  angle which can be detected from Table 7.

The  $\phi$  angle is stable at Camera Station CS 3 with the exception of the January 28 data. If one compares Figure 11 and 12, a rather large (2 cm or 3/4 inch) deviation is shown in the coordinates of point 41 and 42. It can be pointed out, therefore, that the analysis concerning the stability of the orientation matrix provides information about the accuracy of the monitoring.

### 5.3 Accuracy and Correlation of the Parameters

It is an important task of this research project to establish a means which provides information about the accuracy of the obtained results.

There are two approaches to solve this. One is a theoretical and the other is an applied method. The theoretical method calls for substantial computation, namely from the least-squares adjustment of the space intersection. The standard error of the coordinates of points can be computed and using these standard errors, the standard error of the vectors of deflection can be obtained by means of error propagation equations. This solution is elaborate and represents a substan-



Camera Station CS3

Camera Station CS1

Figure 12

Variation in  $\phi$  Angle

tial number of computations along with the problem of proper interpretation.

The applied method is a more direct solution and the interpretation of the result is the same for all the other points. Therefore, this solution has been chosen for this research. The selection of the applied method can further be justified by the substantial changes executed in the methodology and equipment during the monitoring period. These changes were:

- a. Establishment of new control points on the bedrock. (October 12, 1976)
- B. Stabilization of front nodal point of the camera at each camera station. (January 28, 1977)
- c. Establishment of illuminated collimation marks on the camera. (April 12, 1977)
- d. Remeasurement of the control points. (June 10, 1977)
- e. Targeting (with paint) the natural points on the upper wall. (June 10, 1977)

The applied method can be performed in two forms. One is to base the evaluation of the accuracy of the system on actual measurements by establishing control points and using them to compute orientation parameters. The other approach would be a statistical solution by obtaining a best-fitting-curve to each of the individual points and the deviation of a single measurement from that curve would indicate the degree of accuracy achieved. Both of these solutions will be presented here.

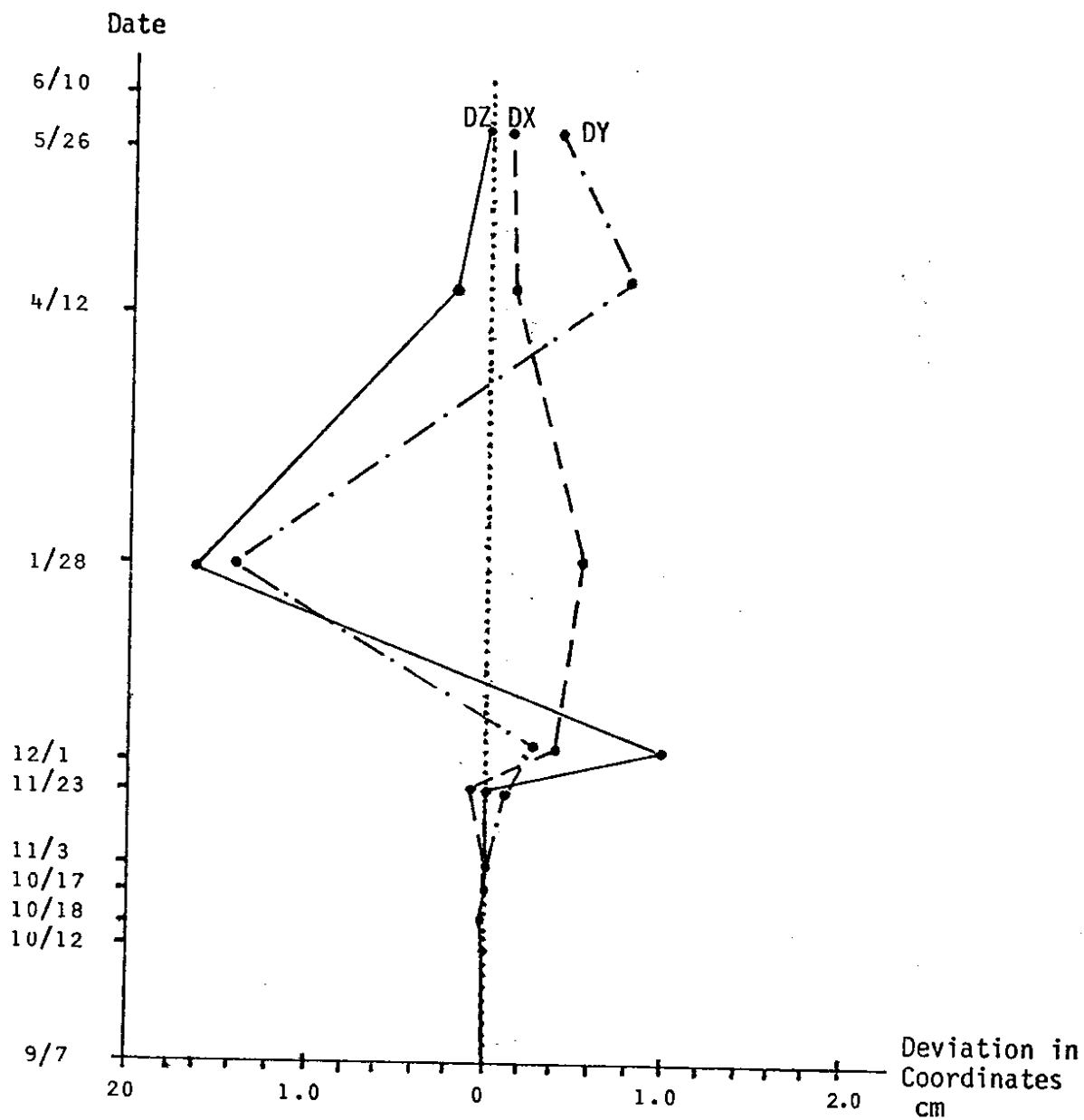


Figure 13  
 Deviation in Coordinates of Control  
 Point 993



The establishment of control or check points or points away from the structure are located in such a way that their positions remain stable during the monitoring. This can be done photogrammetrically as well as by ground survey. The coordinates of these check points are determined similarly to those of the targets. The deviations of the coordinates are also computed similarly. If there were no measuring error, the deviation of the coordinates (DX, DY, DZ) would be zero because there is no change in the position of these points. Thus, any coordinate deviation of the check points represents measuring error and thus, a direct representation of accuracy.

Figure 13 shows an example of the problem. Point 993 was established above the Gabion Wall on bedrock in the form of a painted target. This target was measured each time the monitoring took place. The maximum deviation in the coordinates is about 0.8 cm. Considering the fact that the target is 1040 m (3400 ft.) from the camera stations, this represents a relative accuracy of 1/130,000. This can be regarded as the result of observational errors or other forms of errors inherent in the method. The only exception is the January 28 monitoring where the maximum error is 1.8 cm. This is a clear indication that some other kind of error contributed to these results. Therefore, this measurement may be rejected because this shows a relative accuracy of only 1/58,000 or only 1/3rd as good as that obtained (with the maximum errors) at other monitoring times.

This form of applied method has a further advantage, namely, that the orientation matrices can be computed using these check or control points. The matrices should be computed for each camera

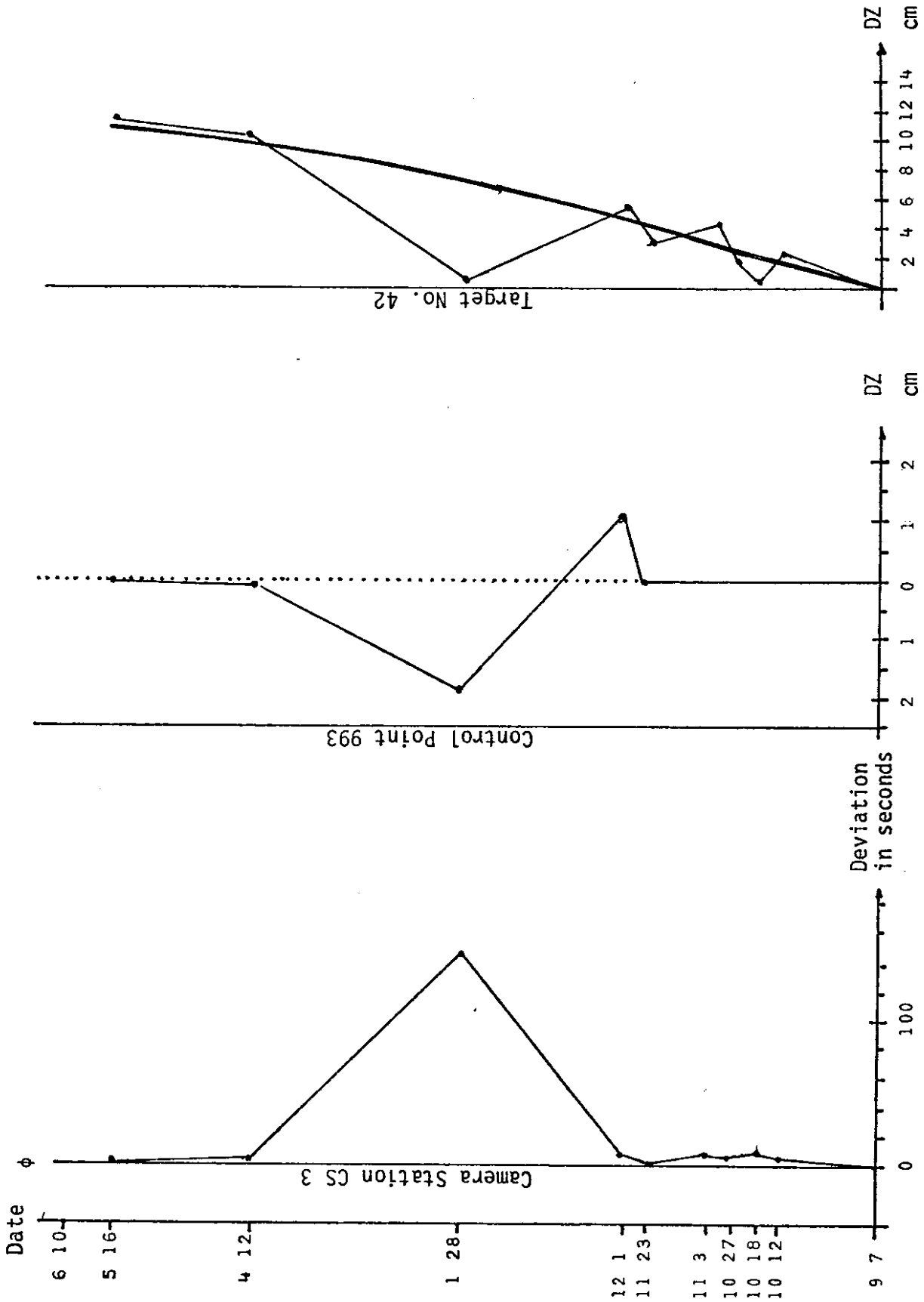


Figure 14

Comparison of Parameters

station every time that the photographs are taken. This will permit the complete analysis of the results by correlating the various parameters. The comparison of the parameters can be done either by inspection of the numerical values of the coordinate deviations [(DX, DY, DZ), ( $\kappa$ ,  $\omega$ ,  $\phi$ ) and (DX, DY, DZ of targets)] and the terms in the orientation matrices or by the comparison using graphical means. As an example of this comparison, Figure 14 is presented where the  $\phi$  orientation angle, DZ coordinate deviation of 993 control point and the deflection (DZ) of target 42 are combined. It can be seen from this figure that a small variation existed in the DZ coordinate of target 42 up to December 1, 1976. This variation is about 1.0 cm which is due to the small change in the camera orientation as shown by the deviation in  $\phi$  angle and only a minor error in observation because there is practically no variation in the DZ of the 993 control point. On the January 28, 1977 line, however, there is a large deviation of more than 2.0 cm in the DZ of target number 42 and nearly 2.0 cm at check point 993. In conclusion it can be said that the January 28 data contains a 2.0 cm error. Consider now the  $\phi$ . The error is due to the change in the camera position. The cause of the change is not precisely known. It could have been caused by the temperature affecting the camera as well as the camera pedestal or by the atmospheric conditions because fog prevailed on that particular day.

The above described method is suitable to evaluate the accuracy each time the monitoring is performed, while the other method which will be described, is more suitable for statistical evaluation of a large

number of monitorings. This method consists of selecting ten points, for example, distributed normally so that they represent the total wall area. The differences between the zero (September 7, 1976) data and that on several other dates of monitoring are plotted. Then a best-fitting-curve is plotted to these data. The discrepancies from the best-fitting-curve is considered as the error of monitoring while the best-fitting-curve is regarded as the indicator of the movement of the wall. The selected points are 8, 16, 18, 41, 42, 43, 44, 60, 67 and 302. In order to simplify the following graphs, the dates are coded as shown in Table 12.

One month is considered to be 30 days. In the following graphs, the date scale is considered as: 1 cm = 1 month.

The accuracy can be estimated from the average deviations which are listed in Table 13 for each point under the  $\sigma_{\Delta x}$ ,  $\sigma_{\Delta y}$ ,  $\sigma_{\Delta z}$  columns for the corresponding coordinates. If the relative accuracy is computed, then the average relative accuracy is 1/85,000. This is in very close agreement with the previous method which is 1/90,000 (the minimum relative accuracy is 1/50,000 and the maximum accuracy is 1/130,000).

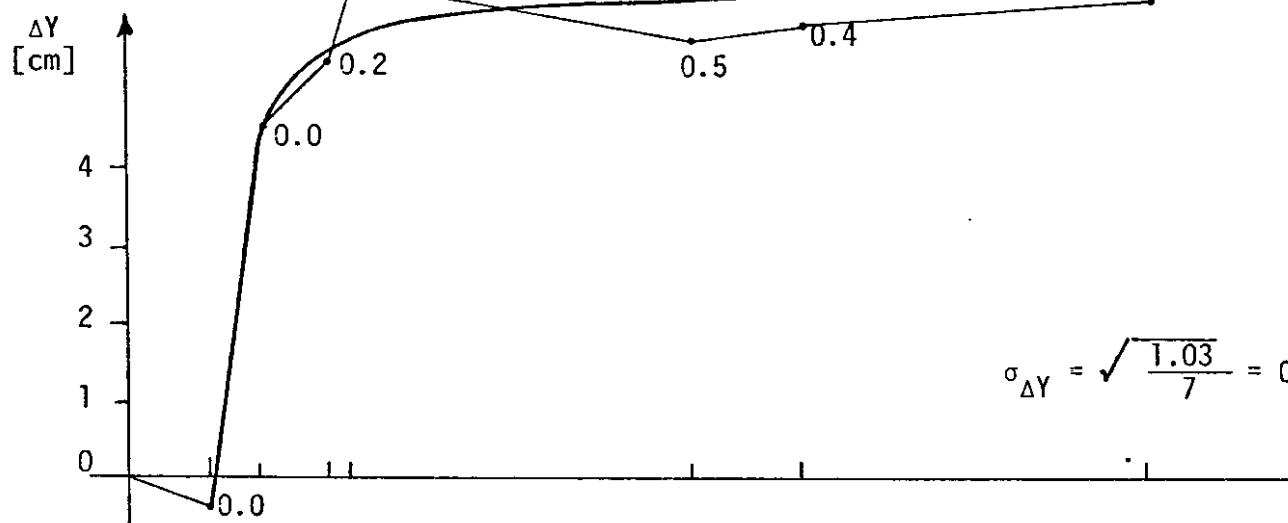
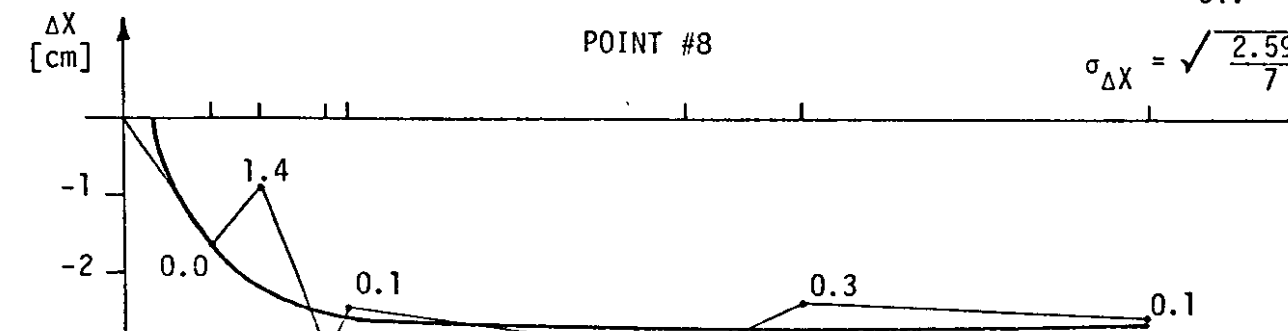
It appears that the first method is more suitable for estimation of accuracy of individual measurements immediately after the photographs are taken. Thus any mistaken measurement can be repeated. The second method, based on the best-fitting curve, is better for the final evaluation. At that time a large amount of data has been collected and therefore, the statistical location of the curve is reliable.

Table 12

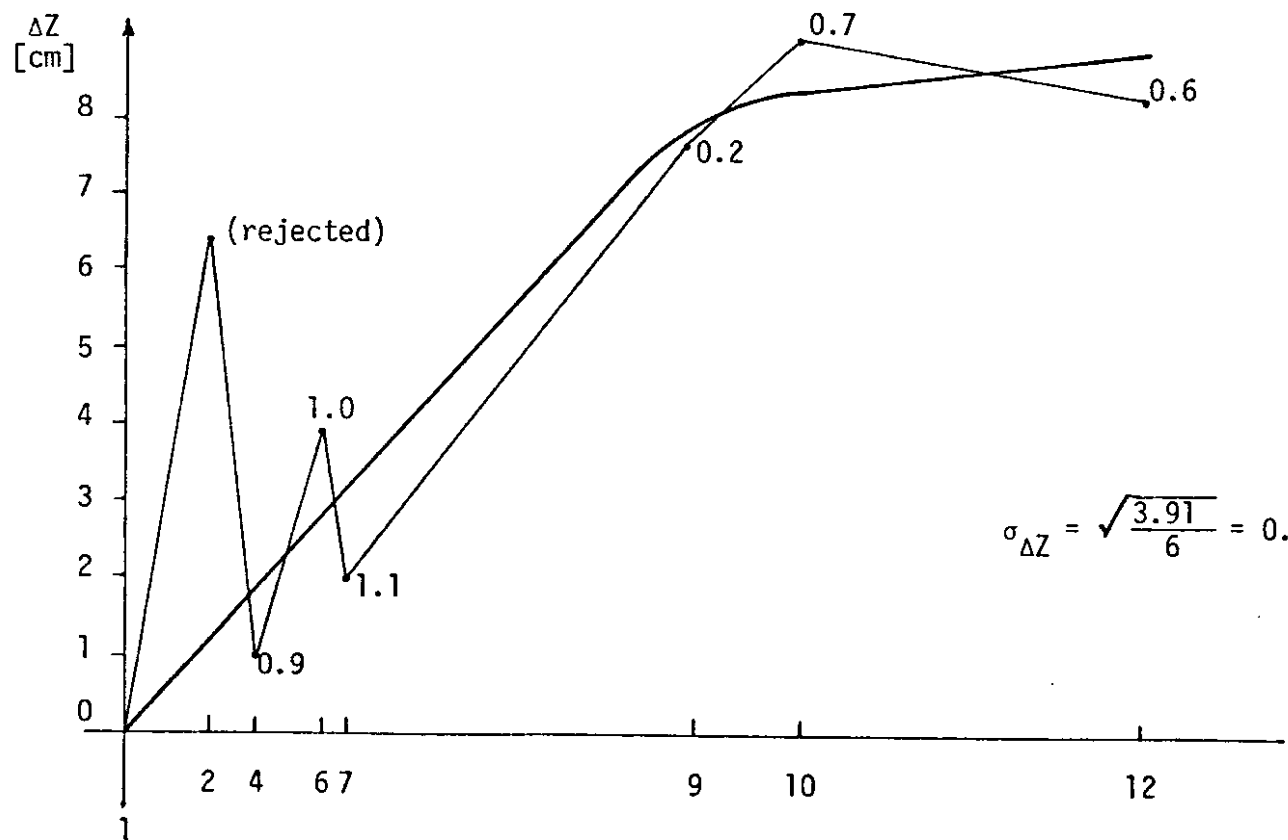
DATE	CODE NUMBER	MONTHS BETWEEN	ORDINATE (Months)
		0.00	
September 7, 1976	1	1.17	0.00
October 12, 1976	2	0.20	1.17
October 18, 1976	3	0.30	1.37
October 27, 1976	4	0.23	1.67
November 3, 1976	5	0.67	1.90
November 23, 1976	6	0.23	2.57
December 1, 1976	7	1.97	2.80
January 28, 1977	8	2.47	4.77
April 12, 1977	9	1.47	7.24
May 26, 1977	10	0.50	8.71
June 10, 1977	11	3.93	9.21
October 6, 1977	12		13.14

POINT #8

$$\sigma_{\Delta X} = \sqrt{\frac{2.59}{7}} = 0.61 \text{ cm}$$

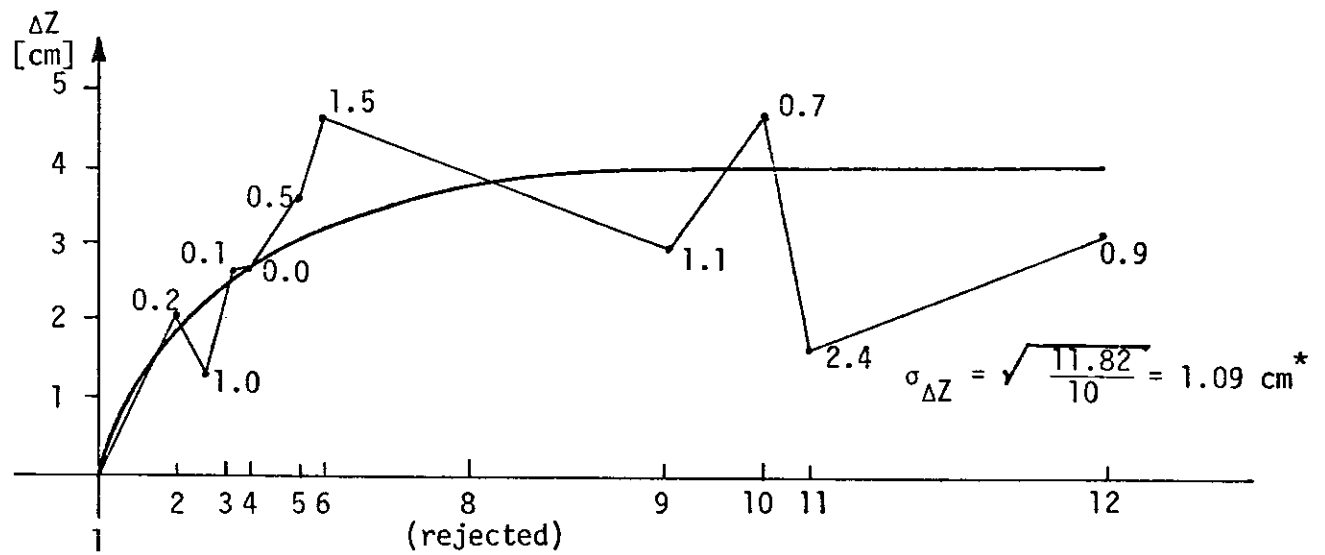
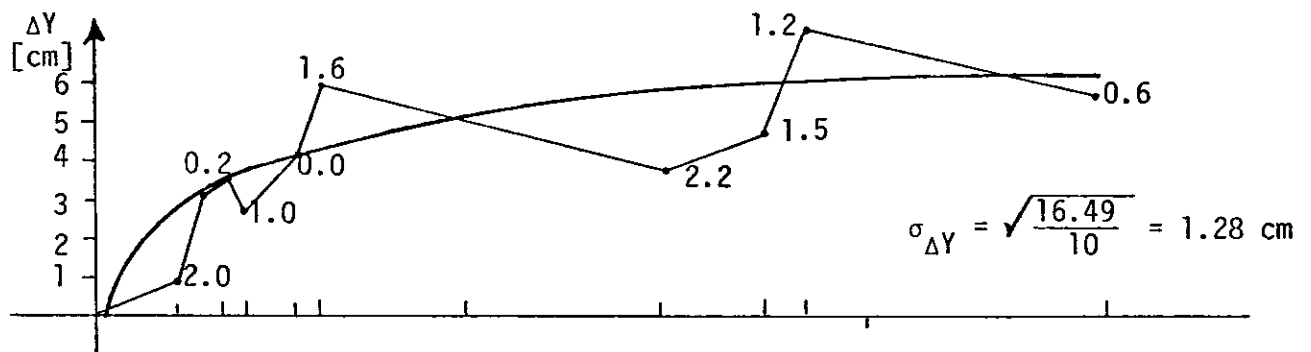
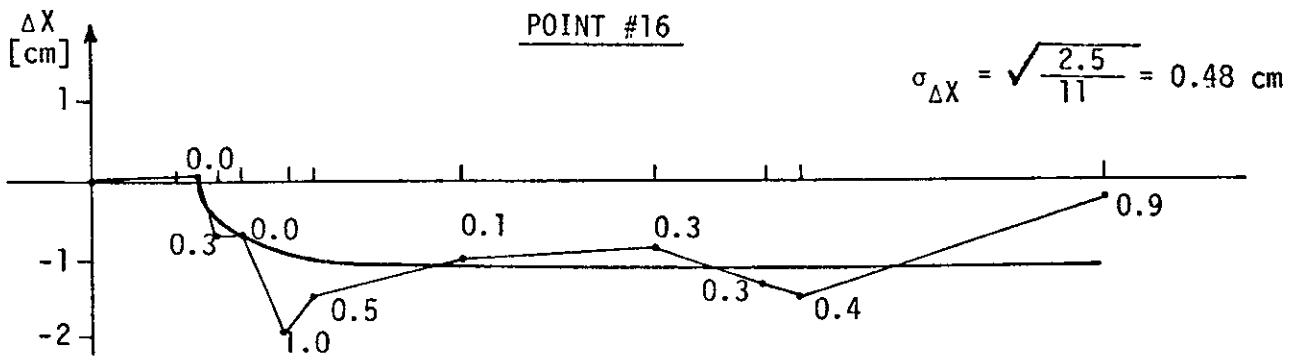


$$\sigma_{\Delta Y} = \sqrt{\frac{1.03}{7}} = 0.38 \text{ cm}$$



$$\sigma_{\Delta Z} = \sqrt{\frac{3.91}{6}} = 0.81 \text{ cm}$$

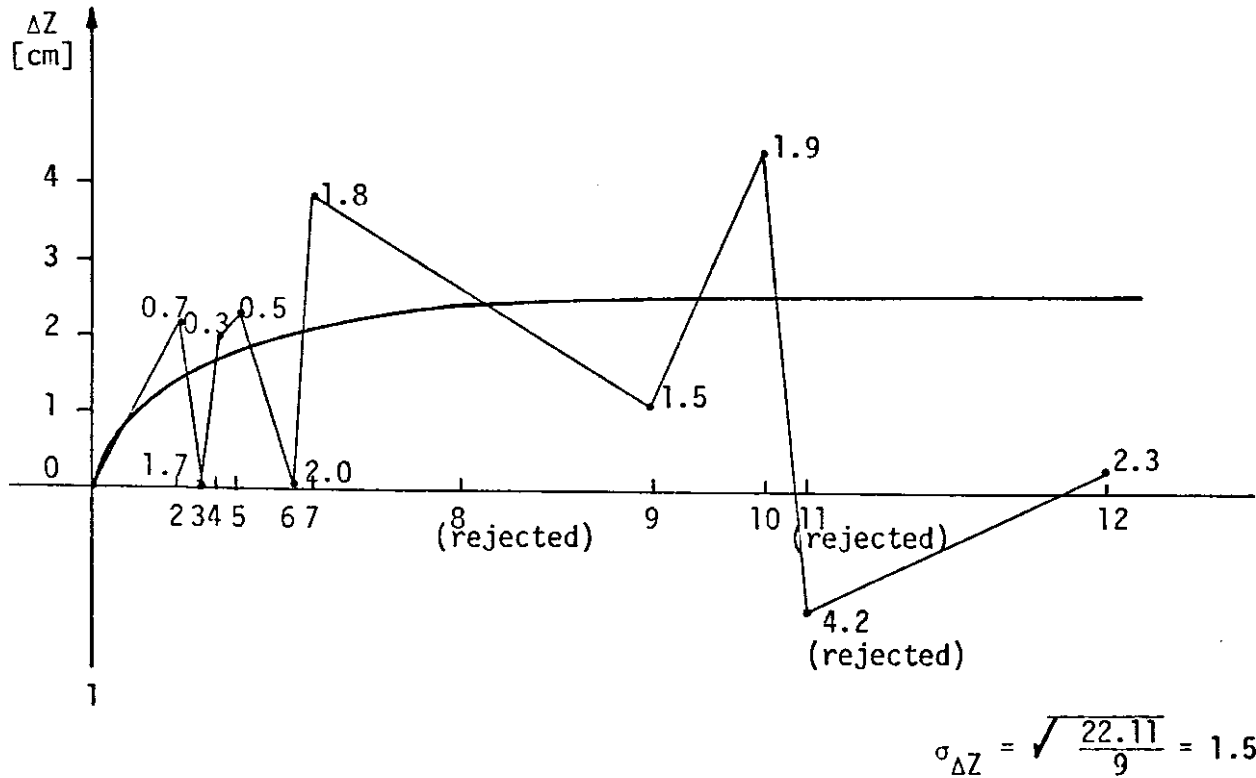
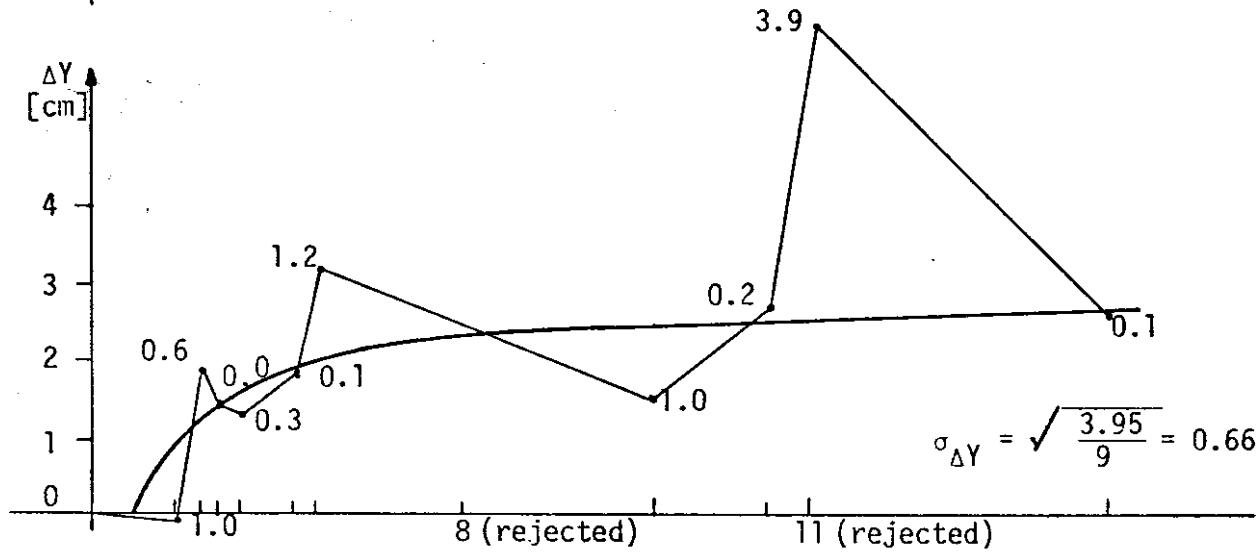
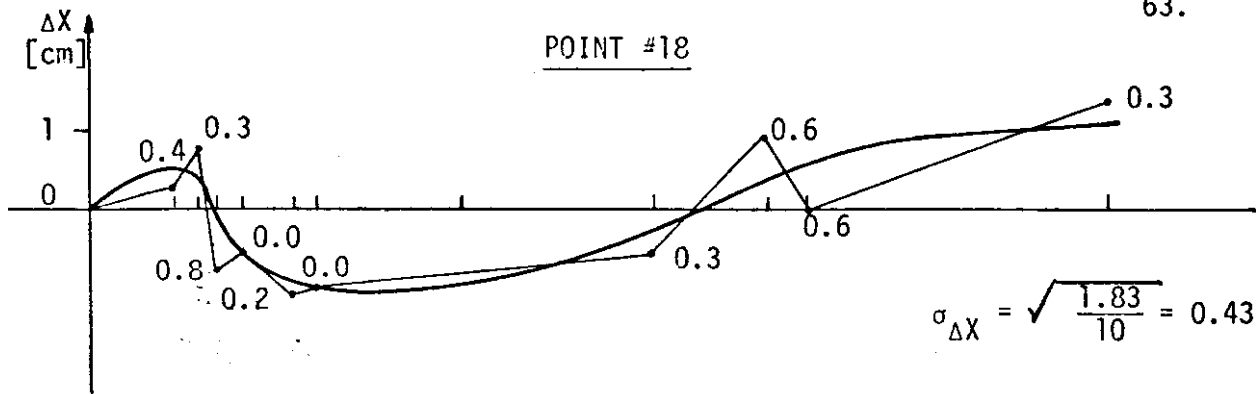
## POINT #16



\* By rejecting the #11 value which is 2.4

$$\sigma_{\Delta Z} = \sqrt{\frac{6.06}{9}} = 0.82 \text{ cm}$$

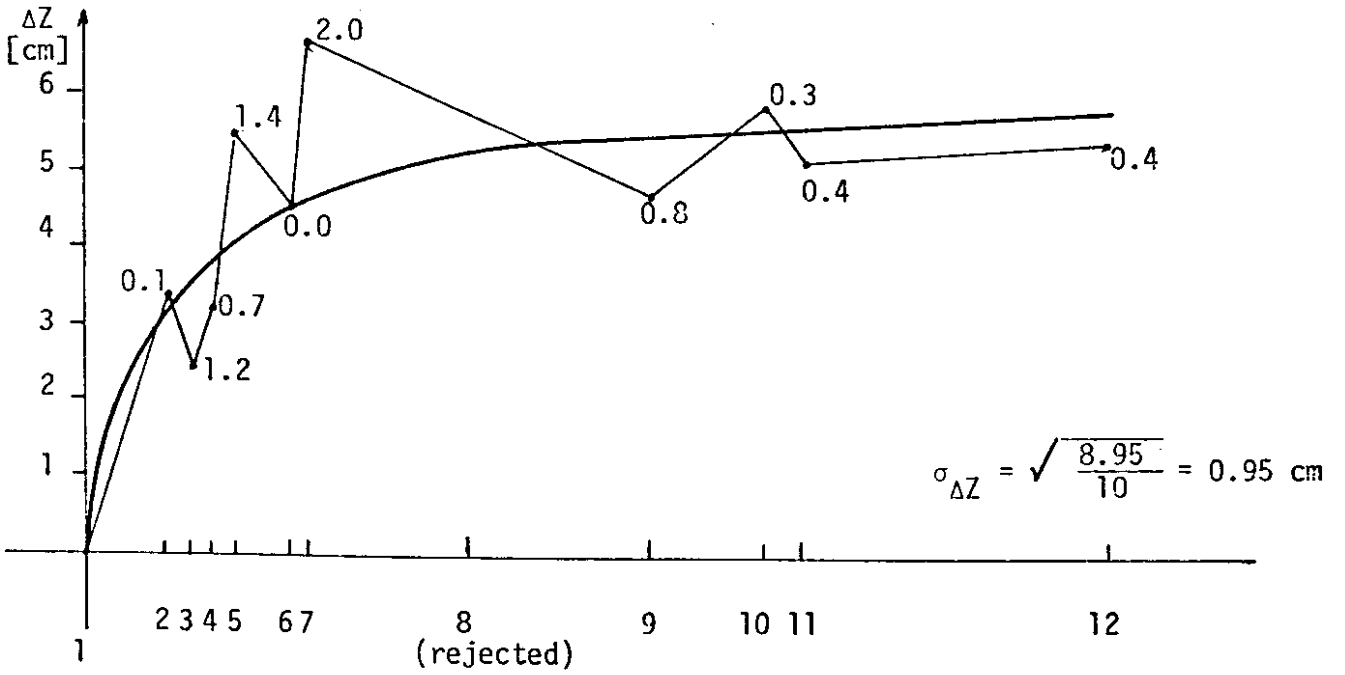
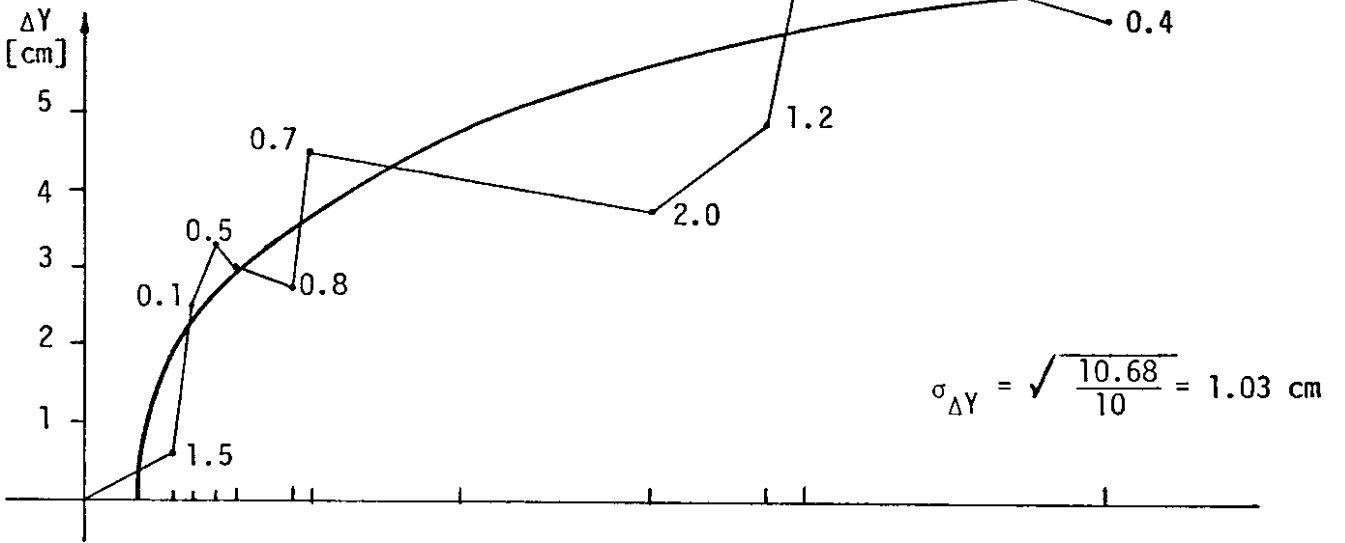
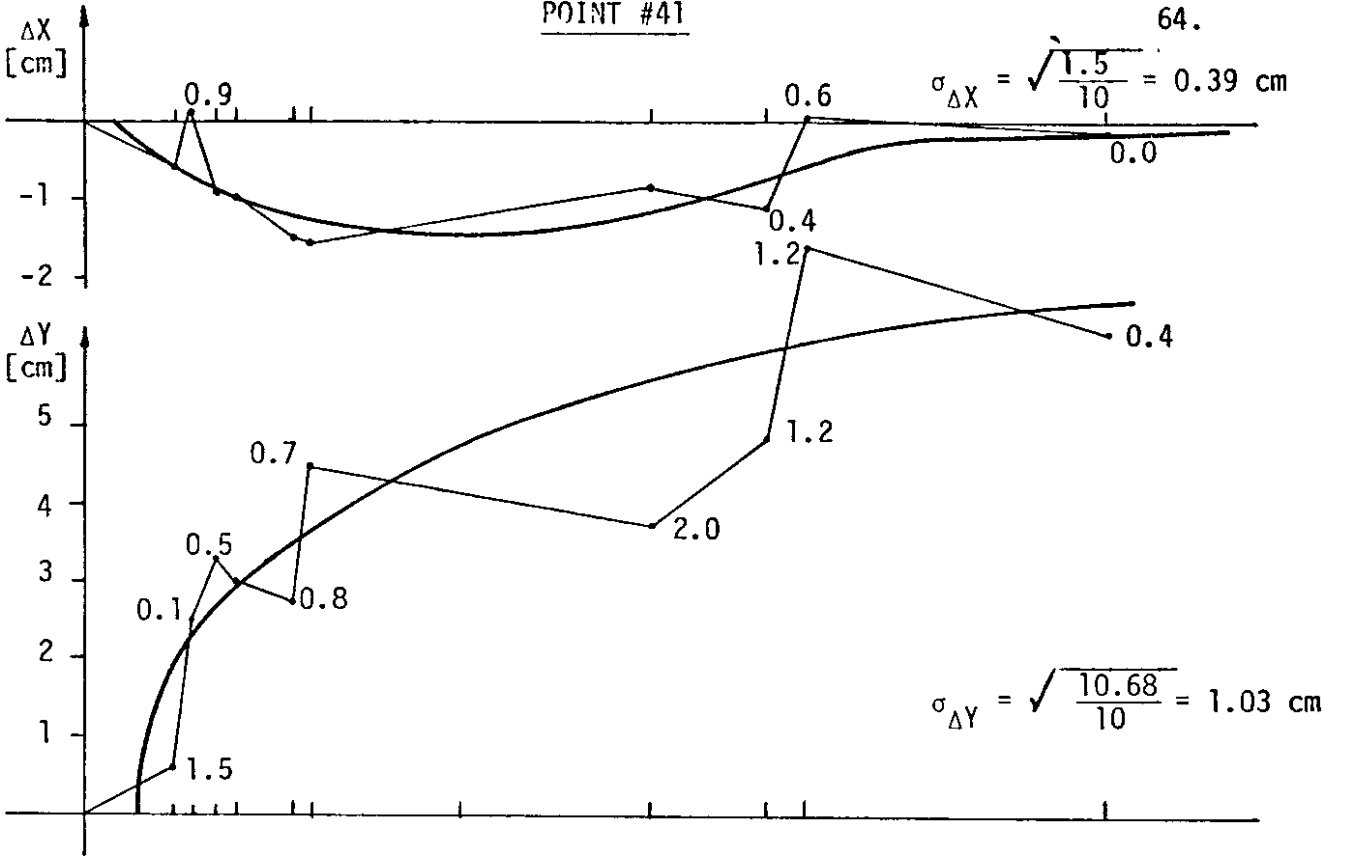
POINT #18





POINT #41

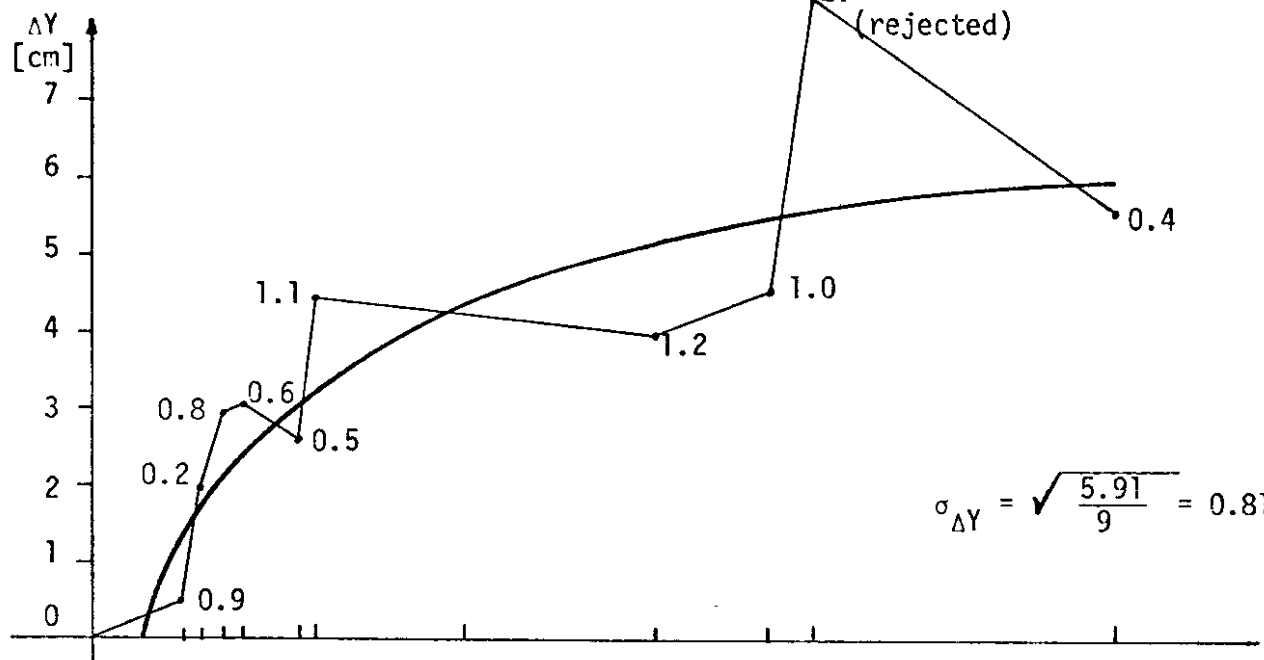
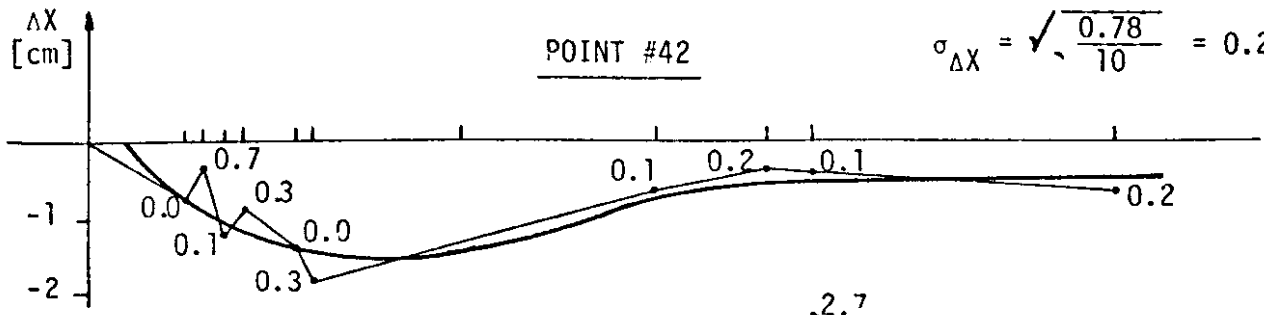
64.



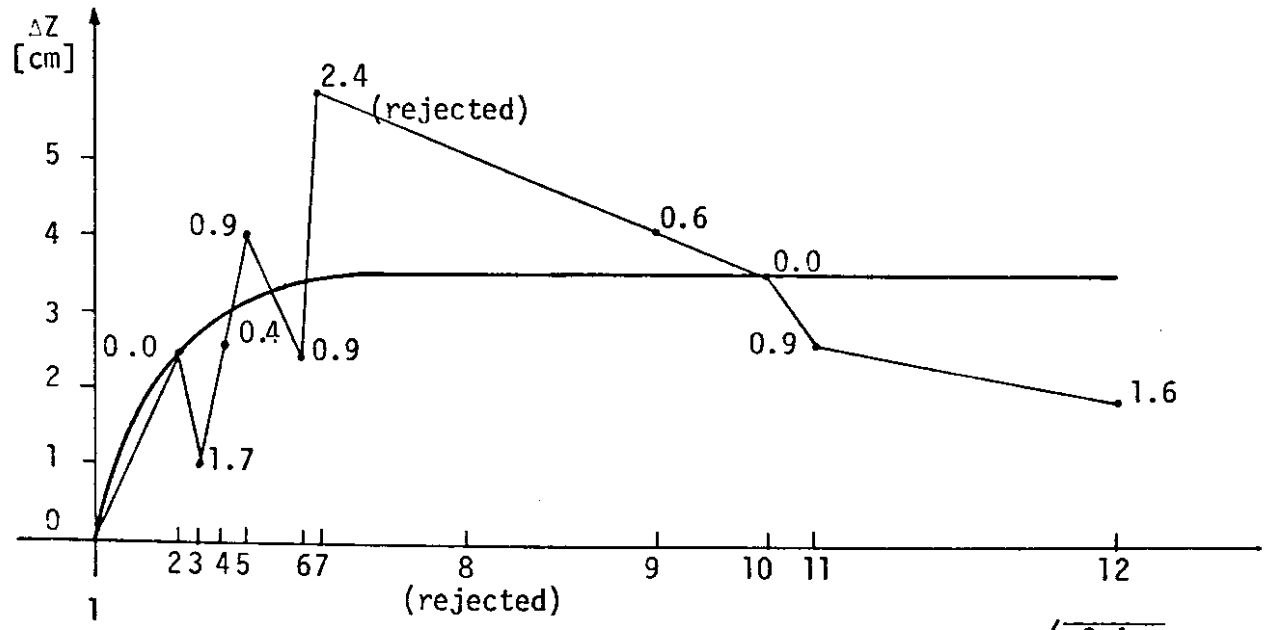
8 (rejected)

POINT #42

$$\sigma_{\Delta X} = \sqrt{\frac{0.78}{10}} = 0.28 \text{ cm}$$



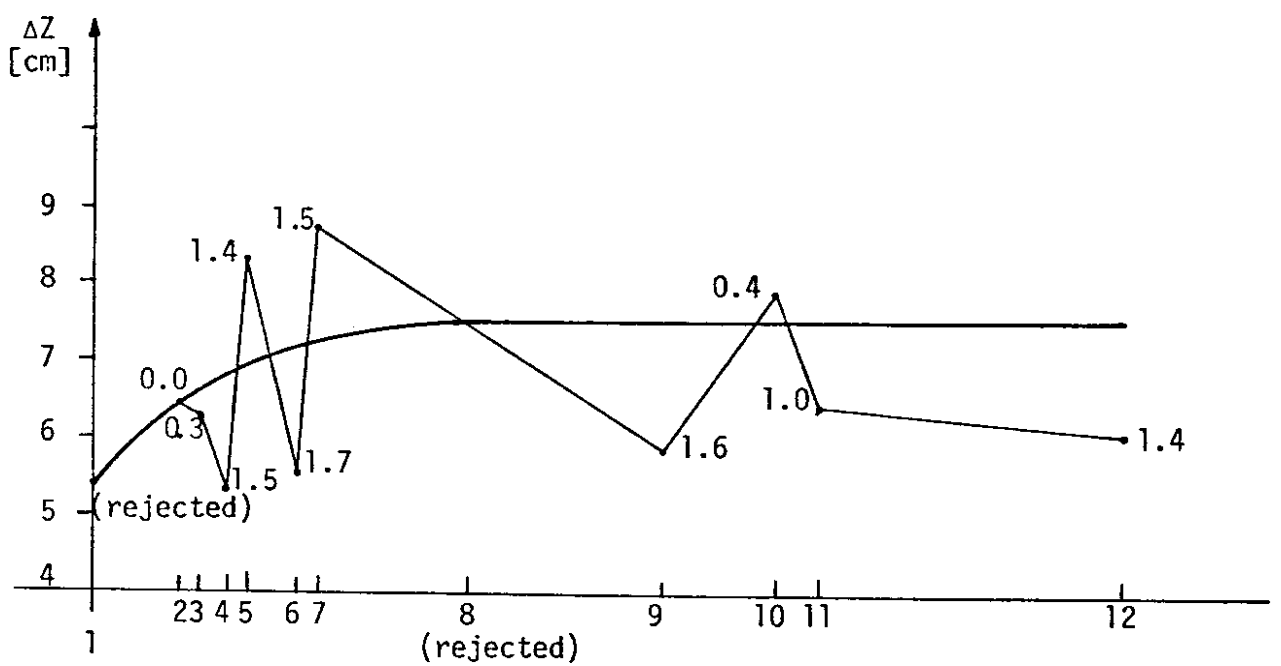
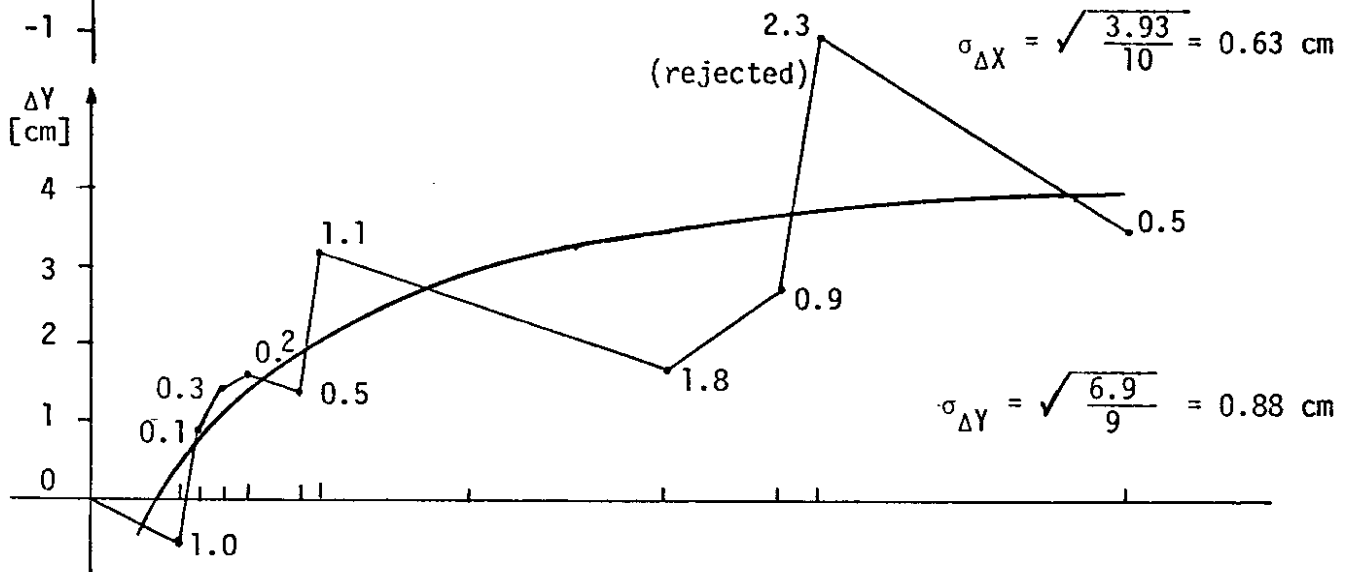
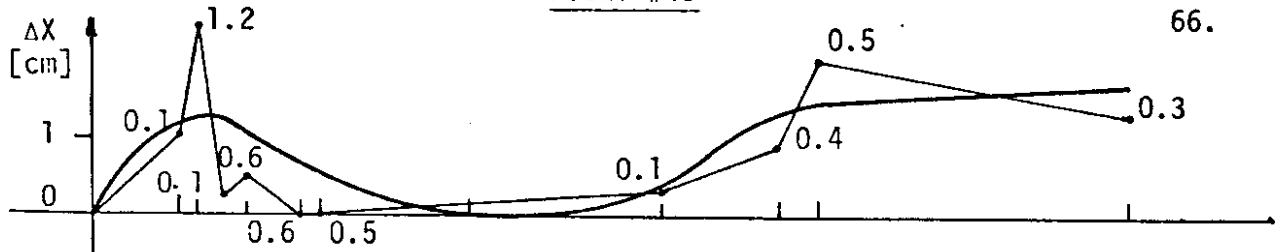
$$\sigma_{\Delta Y} = \sqrt{\frac{5.91}{9}} = 0.81 \text{ cm}$$



$$\sigma_{\Delta Z} = \sqrt{\frac{8.4}{9}} = 0.97 \text{ cm}$$

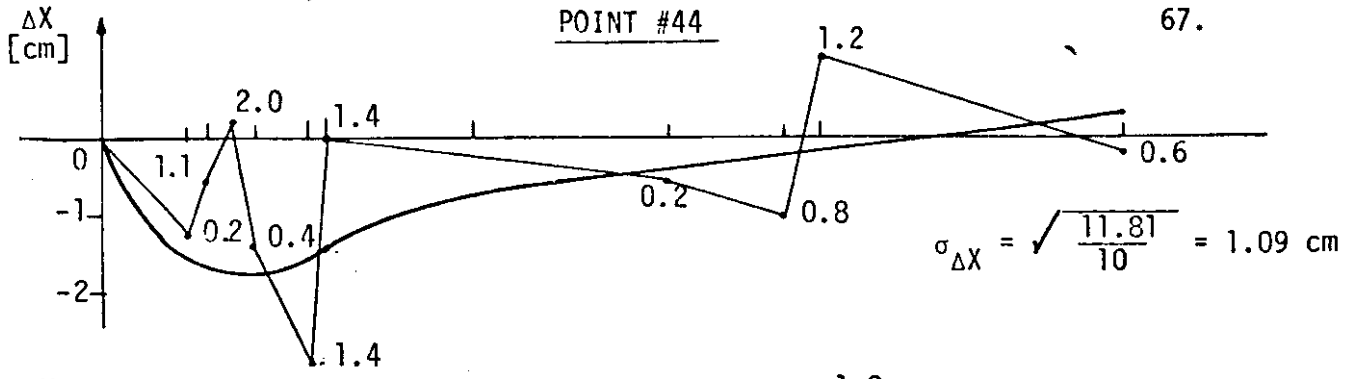
POINT #43

66.

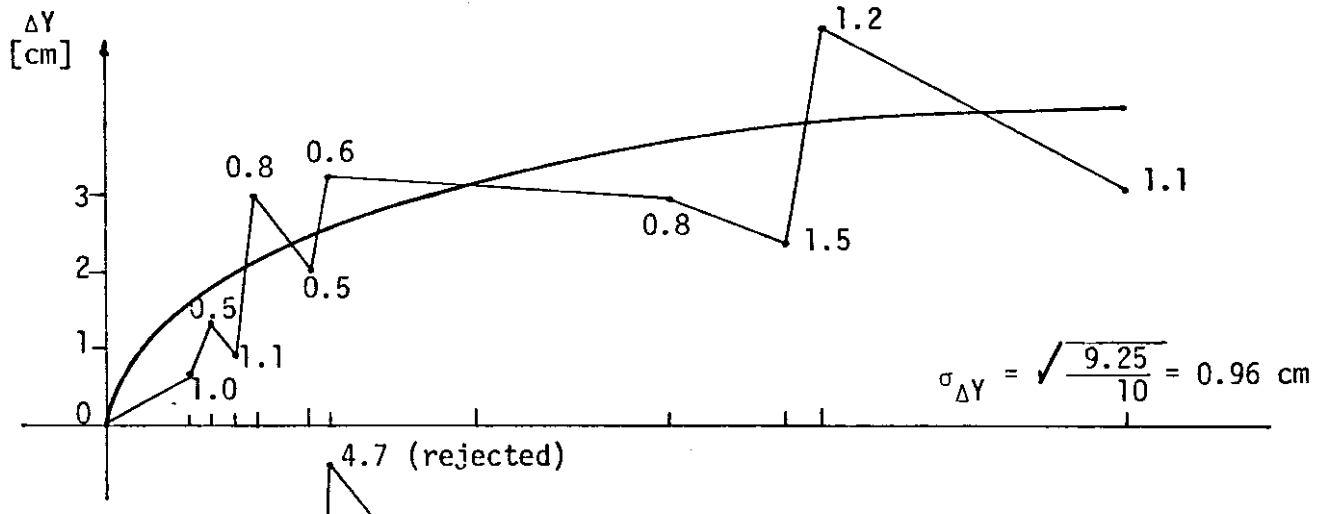


POINT #44

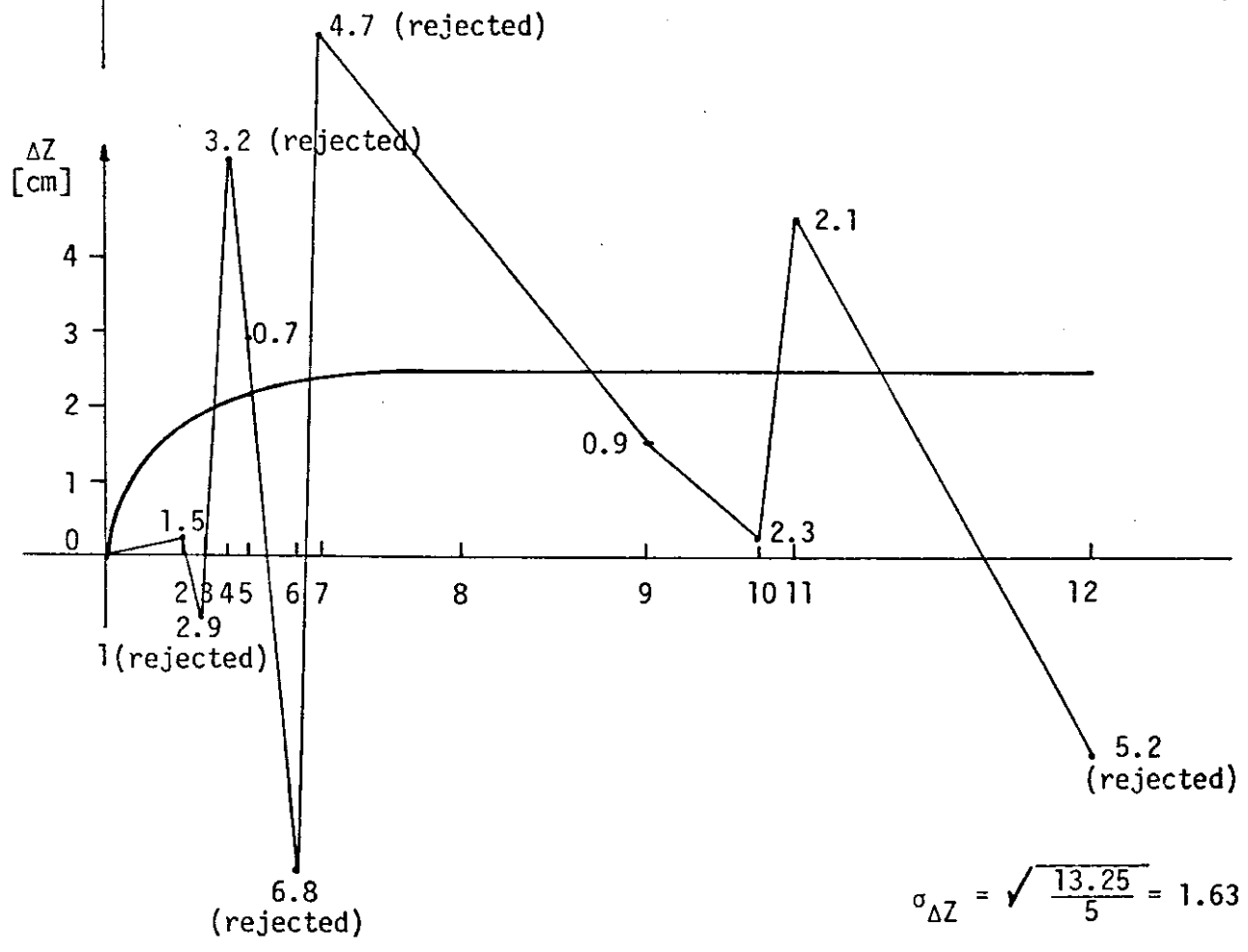
67.



$$\sigma_{\Delta X} = \sqrt{\frac{11.81}{10}} = 1.09 \text{ cm}$$



$$\sigma_{\Delta Y} = \sqrt{\frac{9.25}{10}} = 0.96 \text{ cm}$$

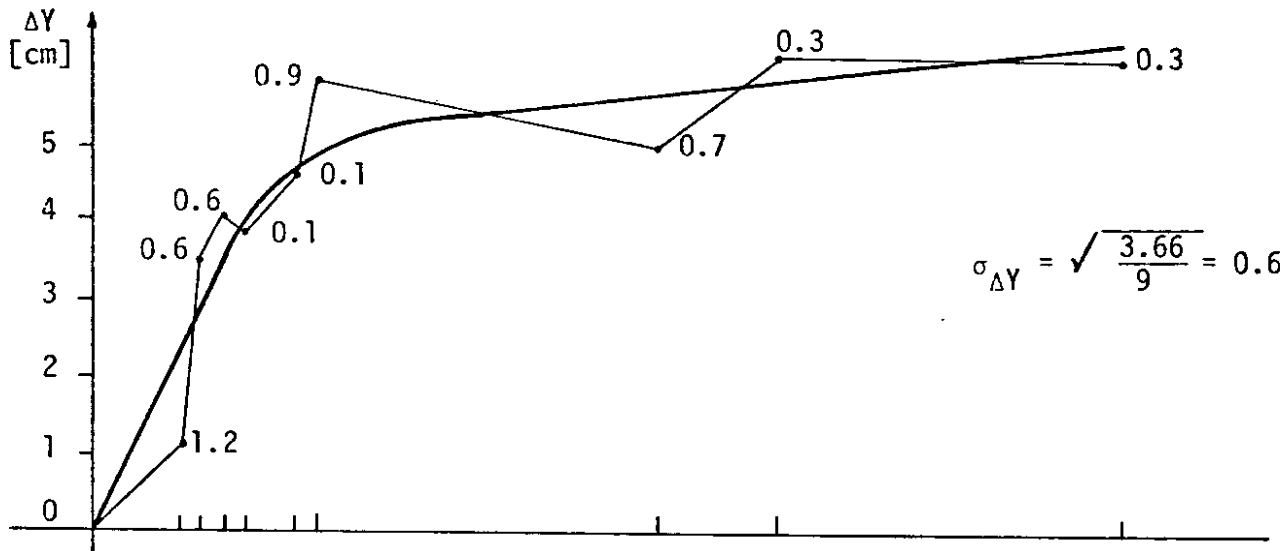
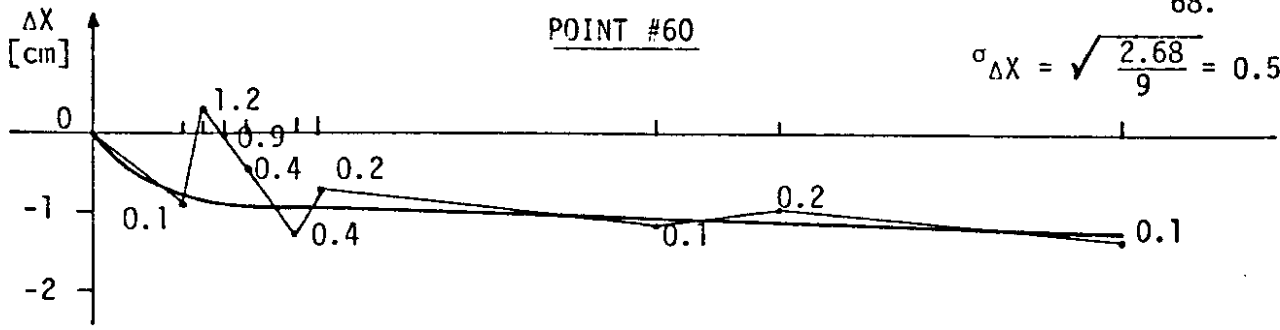


$$\sigma_{\Delta Z} = \sqrt{\frac{13.25}{5}} = 1.63 \text{ cm}$$

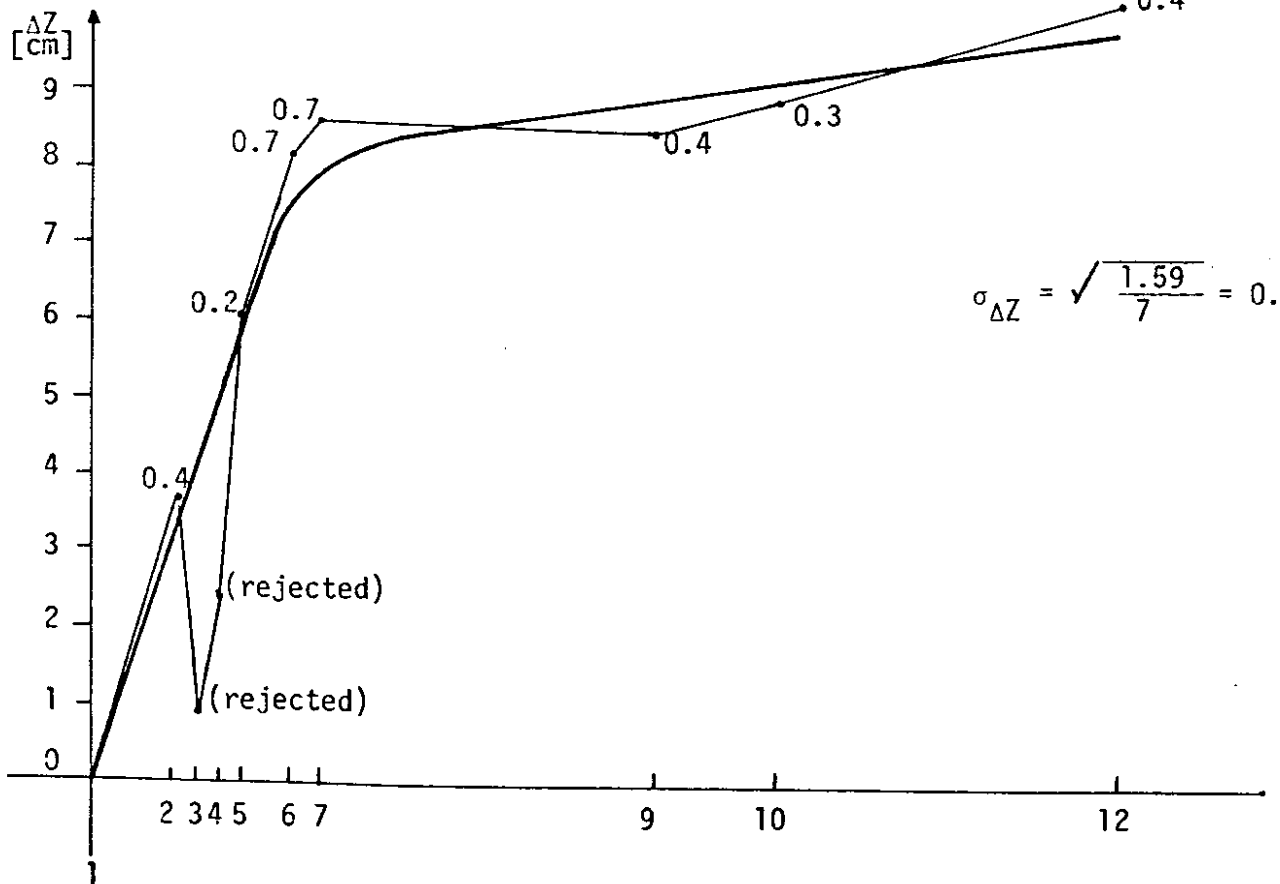
POINT #60

68.

$$\sigma_{\Delta X} = \sqrt{\frac{2.68}{9}} = 0.55 \text{ cm}$$



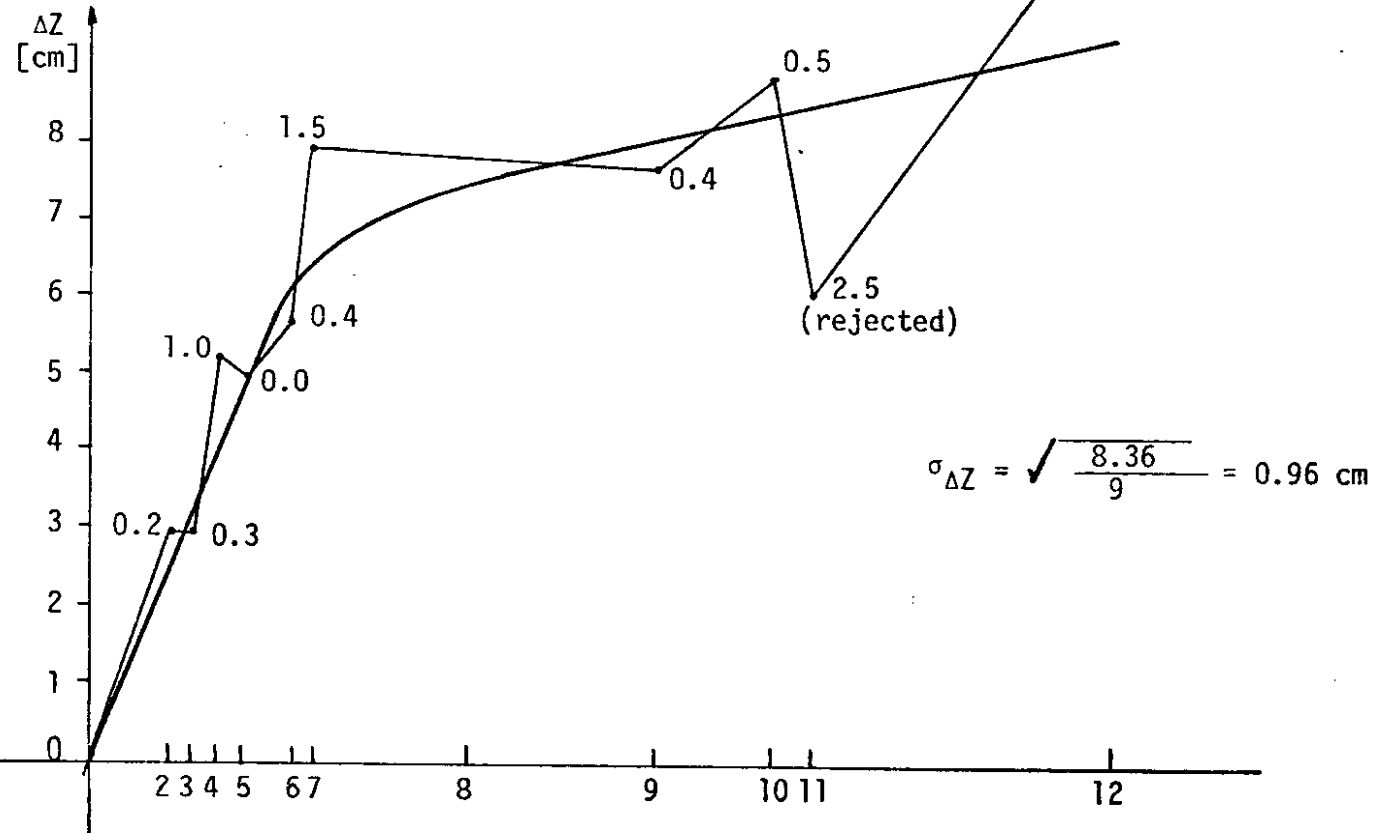
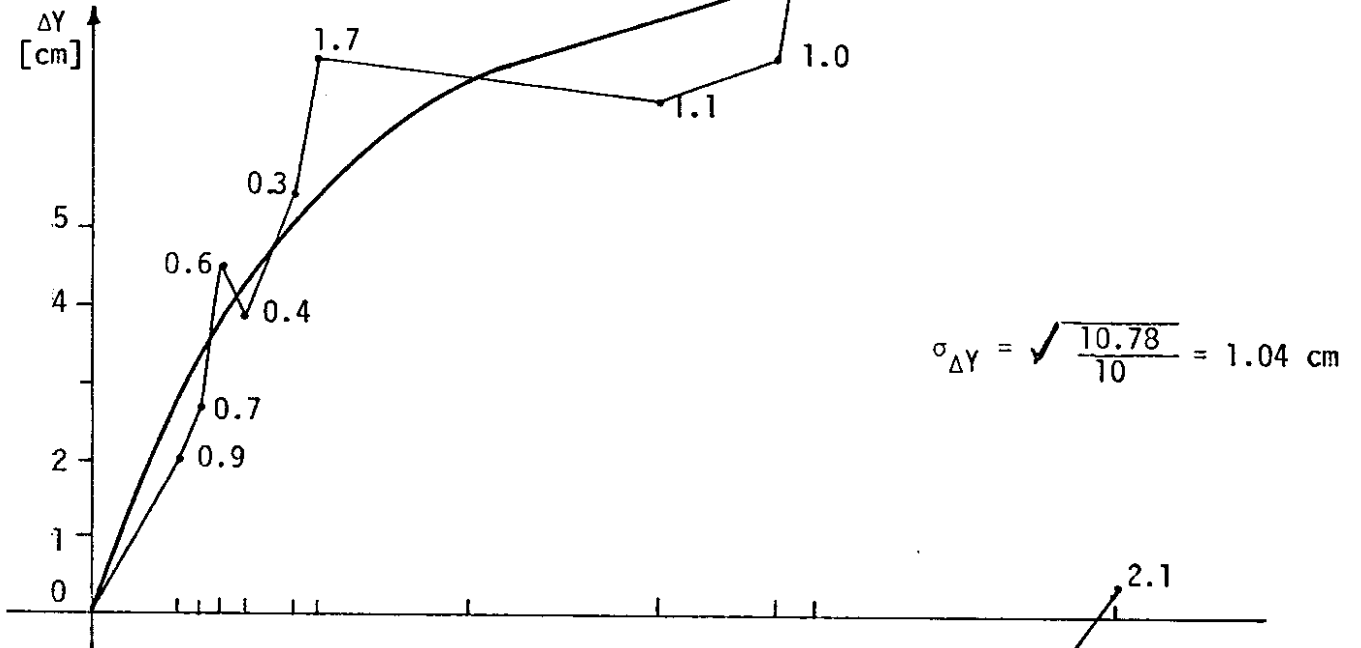
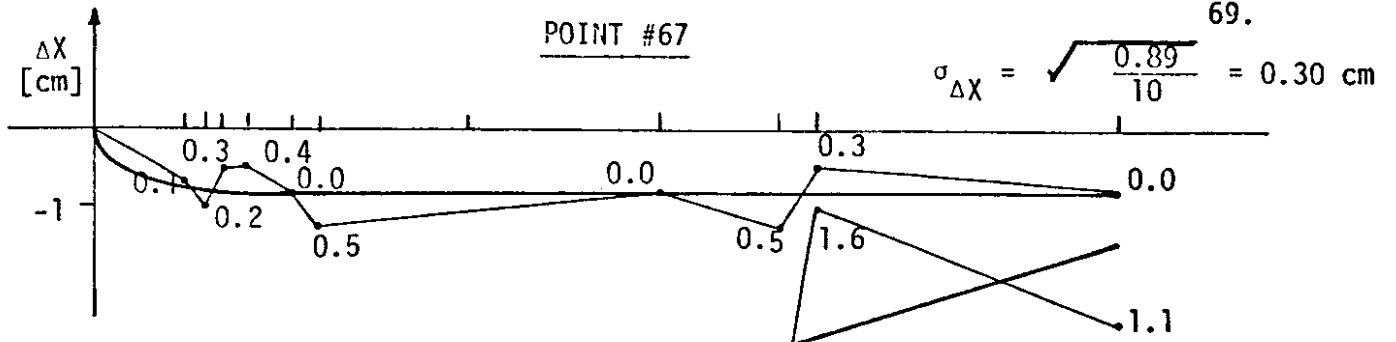
$$\sigma_{\Delta Y} = \sqrt{\frac{3.66}{9}} = 0.64 \text{ cm}$$



$$\sigma_{\Delta Z} = \sqrt{\frac{1.59}{7}} = 0.48 \text{ cm}$$

POINT #67

69.



POINT #302

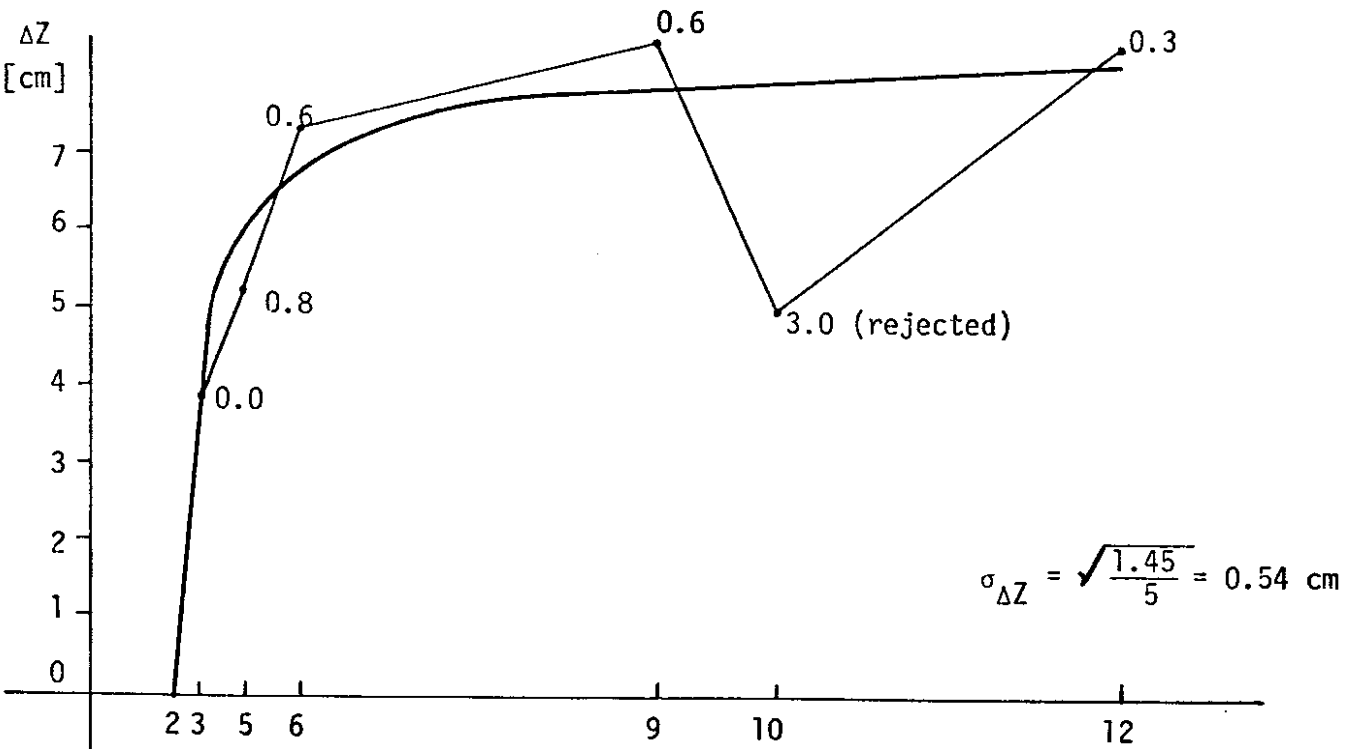
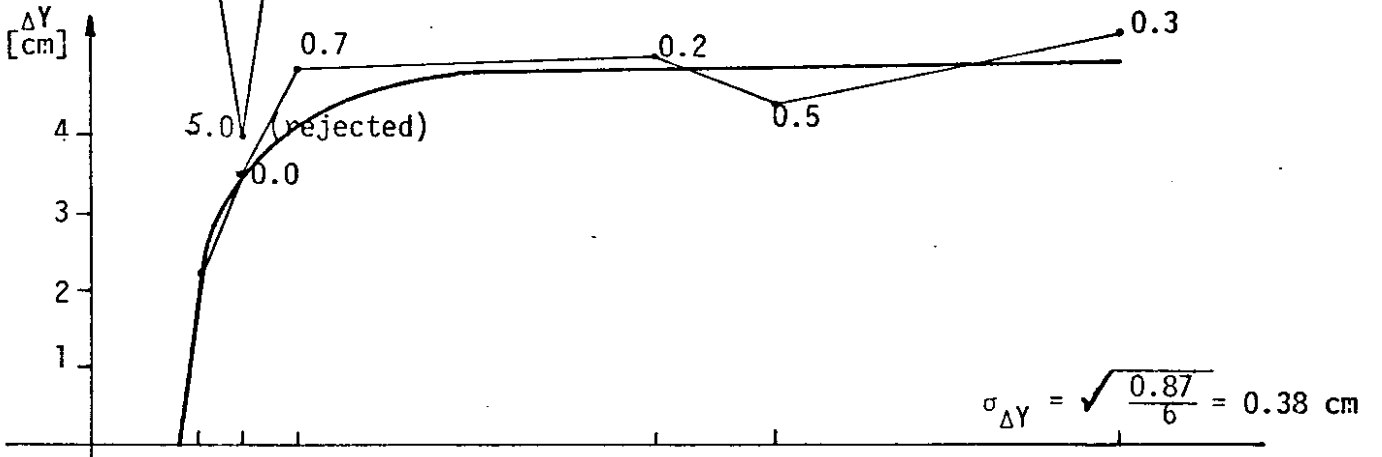
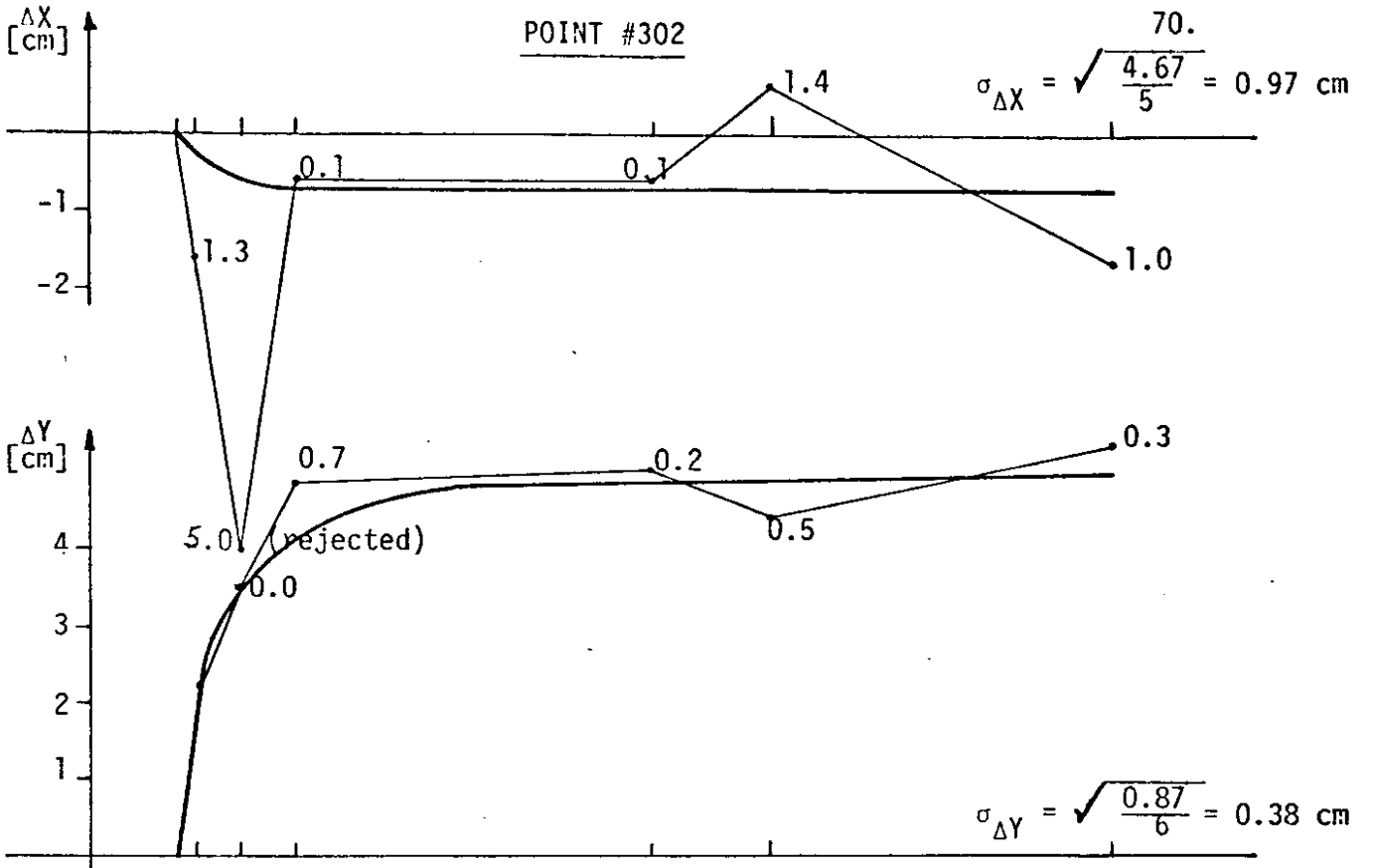


Table 13

ACCURACY RESULTS

POINT #	$\sigma_{\Delta x}$	$\sigma_{\Delta y}$	$\sigma_{\Delta z}$
8	0.61	0.38	0.81
16	0.48	1.28	0.82
18	0.43	0.66	1.57
41	0.39	1.03	0.95
42	0.28	0.81	0.97
43	0.63	0.88	1.30
44	1.09	0.96	1.63
60	0.55	0.64	0.48
67	0.30	1.04	0.96
302	0.97	0.38	0.54
Average	5.7 mm	8.1 mm	10.0 mm

Estimated Accuracy:

$$\sigma_{\Delta x} = \pm 5.7 \text{ mm}$$

$$\sigma_{\Delta y} = \pm 8.1 \text{ mm}$$

$$\sigma_{\Delta z} = \pm 10.0 \text{ mm}$$

Assuming the photographic distance is 850 m, then the accuracy is 1/85,000.



There were a number of technical changes executed during the monitoring period. Two of these were the most influential. They are the illumination of the collimation marks and the remeasurement of the control points.

The illumination of the collimation marks changed the calibration of the marks by about 40 micrometers. This also influenced the achieved accuracy. The results obtained after April 12, 1977 were better by a very small amount than the previous values. This was accomplished by the use of affine transformation to obtain the photo coordinates from the comparator (or machine) coordinate. Previously conformal transformation was used which gives lesser accuracy. However, the difference is not significant.

The second most influential change was the remeasurement of control points and the change of control points from one date of photography to another. The remeasurements of the control points affects the results dated after June 10, 1977. The accuracy of the control or check points affects the orientation matrices but the geometry of the check points also has considerable influence. As a consequence, it is desirable to use the same check points for each camera station in order to obtain the best possible correlation among the various monitored data. Three control points were used (992, 993 and 884) for each plate. While the first two control points are recognizable on each plate, the third one is not identifiable on the plates made September 7, 1976, November 3, 1976 and November 23, 1976. The results of these dates are not correlatable in this form with the rest of the data. In order to over-

come this difficulty the fictitious positions of point 834 were computed on these photographs. By doing so, a good correlation was achieved among all the plates using those positions to perform a uniform computation.

#### 5.4 Conclusions and Recommendations

The photogrammetric monitoring method is capable of providing the spatial positions of a large number of points.

It is an external monitoring method and as such will register surface movement in three dimensional space. Considering the presently known external monitoring methods, the photogrammetric method is the most economical; that is, the least amount of dollar expenditure occurs per point monitored.

Among the presently developed methods, this one proved to be the most economical and the least time consuming. The accuracy of this newly developed method is the same, or in most cases, superior to the previous ones. While the previous methods give a relative accuracy between 1/48,000 and 1/94,000 of the photographic distance, this method provided between 1/50,000 and 1/150,000.

A further advantage of the method is that the camera stations are remotely located from the structure. Thus they are not affected by vibration and other disturbances which inevitably occur during construction by the traffic of heavy machinery, etc.

The method appears to be best suited for large structures and is universally applicable to different types of structures such as retaining walls, buildings, bridges, etc.

The basic disadvantage of the method developed is the instability of the camera stations and the rather large transportation weight of the camera (120 lbs.). To overcome this difficulty, it is recommended that three camera cones be used and these cones permanently mounted to the stations. Only the camera magazine should be changed during the monitoring. The method would remain economical in spite of the extra camera cones because a cone costs about \$650.

Further, it is not recommended that a rotatable camera station be used in the future due to the inherent instability of the system. If no other possibility exists for complete photographic coverage of the structure, a shorter focal length cone, such as  $f = 305 \text{ mm}$  or 12" should be used.

For future monitoring procedures the following work flow is recommended:

1. Reconnaissance and design of photogrammetric and control survey system
  - 1.1 Camera stations should be designed for  $60^\circ$  parallax angles.
  - 1.2 Specifications for control survey of the base lines should be accurate within  $\pm 2 \text{ mm}$  and angles within  $\pm 3$  inches.
2. Establishment of camera stations
  - 2.1 Camera stations should be established on bedrock free of disturbances such as vibrations, etc.
  - 2.2 They should be permanently located with camera cones and water-proof housing.

3. Targeting the structure
  - 3.1 Targets should be anchored to the structure so that they represent the motion of the structure.
  - 3.2 The targets should be balls whenever feasible and thus, they would not exhibit elliptical images.
4. Ground control survey
  - 4.1 Determination of camera station coordinates
  - 4.2 Reduction of coordinates to the frontal nodal point of the camera.
  - 4.3 Determination of orientation elements ( $\phi$ ,  $\omega$ , and  $\kappa$  angles) for each camera station.
5. The "zero date" photographs
  - 5.1 The "zero date" photographs should be taken so that two photographs are exposed for each camera station and every target on each photograph should be observed five times on comparator or comparable photogrammetric instrument. This way a complete reliable data can be established.
  - 5.2 At least 4-5 check or control points should be established and located in firm positions independent of the structure.
6. Take photographs at predetermined intervals.
7. Observation of the negatives
  - 7.1 The number of observations should be four for the collimation marks and two for the targets.

7.2 The standard error of the observation at the collimation marks should not exceed  $\pm 6 \mu\text{m}$ .

7.3 Compute and print the standard errors of the coordinates of the collimation marks and target points.

8. Computation of coordinates

8.1 Using the predetermined orientation elements compute the coordinates of the targets and check points and compare to the "zero data."

8.2 Compute the orientation matrix and the  $\phi$ ,  $\omega$  and  $\kappa$  angles.

9. Analysis and tabulation of the results.

The following changes or new research are recommended:

The observation of the plate coordinates and the collimation marks should be recorded along with their standard error in order to analyze the overall accuracy. This will provide general information about the compatibility of the photographs made at various times with respect to the weather, visibility conditions and photographic processing, etc.

The orientation elements should be computed for each time in order to check the positional accuracy of the camera stations. This would give information for the general acceptability of the photographs. If required, they could be retaken. Therefore, there would not be a gap in the monitoring time.

An evaluation method such as one with a best-fitting-curve should be used for intermediate and final analysis of the results. This analysis should be done point by point and criterion for rejection of mistaken data should be established.

Finally, this research project should continue to arrive at a universal solution whereby a monitoring system is established. This monitoring system should be applicable for any form of structure using terrestrial, aerial or the combination of the two kinds of photographs.

### 6.0 REFERENCES

- American Society of Photogrammetry, "Manual of Photogrammetry," The American Society of Photogrammetry, Third Edition, Washington, D. C., 1966.
- Borchers, P. E., "The Photogrammetric Study of Structural Movements in Architecture," Photogrammetric Engineering, Vol. 30, No. 5, p. 809-817, 1964.
- Brandenberger, A. J., "Aerial Triangulation for Ohio Highways Department Surveys and Right-of-Way Acquisition," Technical Reports 1, 2, 3, 4, The Ohio State University Research Foundation, Columbus, Ohio, 1964.
- Brandenberger, A. J., "Aerial Triangulation by Least Squares," Mapping and Charting Research Laboratory, First, Second, Third, Fourth Interim, and Final Technical Reports. The Ohio State University Research Foundation, Columbus, Ohio, 1961.
- Brandenberger, A. J., "Economic Considerations in Engineering Photogrammetry," Ninth Annual Photogrammetry Short Course, Illinois, 1969.
- Brandenberger, A. J., "Fehlertheorie der Äusseren Orientierung von Steilaufnahmen," Eidg. Technische Hochschule, Zurich, 1957.
- Brandenberger, A. J. and Erez, M. T., "Photogrammetric Determination of Displacement and Deformations in Large Engineering Structures," Canadian Surveyor, Vol. 26. No. 2, 1972.
- Brock, R. H., "Preliminary Results in Image Measurement Precision Vs. Image Contrast and Background Density Combinations," Computational Photogrammetry Symposium, p. 1-9, 1969.
- Brown, D. C., "Advanced Methods for the Calibration of Metric Cameras," Computational Photogrammetry Symposium, p. 96-213, 1969.
- Davis, Raymond E. and Foote, F. S., "Surveying Theory and Practice," Fourth Edition.
- DeGross, G. E., "A Study of Terrestrial Methods for Determining the Motion in Structural Highway Design," Thesis, University of Washington, 1970.
- Erez, M. T., "Analytical Terrestrial Photogrammetry Applied to the Measurement of Deformations in Large Engineering Structures," Dissertation, University of Laval, 1971.
- Erlandson, J. P., Peterson, J. C. and Veress, S. A., "Performance of Observations of Structural Deformations by Photogrammetric Methods," Technical Report, U. S. Army Corps of Engineers, Seattle District, 1973.

- Erlandson, J.P., Peterson, J. C. and Veress, S. A., "The Modification and Use of the BC-4 Camera for Measurements of Structural Deformation," Proceedings of the American Society of Photogrammetry, Fall Convention, September 10-13, 1974.
- Erlandson, J.P. and Veress, S. A., "Contemporary Problems in Terrestrial Photogrammetry," Photogrammetric Engineering and Remote Sensing, 1974.
- Erlandson, J.P. and Veress, S. A., "Photogrammetrische Erfassung von Bauwerksveränderungen," VR-Vermessungswesen und Raumordnung, Heft 8/1976.
- Erlandson, J.P. and Veress, S. A., "Monitoring Deformations of Structures," Photogrammetric Engineering and Remote Sensing, Vol. 41, No. 11, Nov. 1975, pp. 1375-1384.
- Erlandson, J. P. and Veress, S. A., "Methodology and Standards for Structural Surveys," Proceedings of the Symposium on Close-Range Photogrammetric Systems, July 28-August 1, 1975, pp. 575-595.
- Finsterwalder, R., "Erfahrung mit der Stereokartierung bei affin verzerrten Strahlenbündeln," Deutsch. Geod. Kom. Bul. 4., München, 1963.
- Faig, W., "Vermessung dünner Seifenlamellen mit Hilfe der Nahbereichsphotogrammetrie," Verlag der Bayerischen Akademie der Wissenschaften, München, pp. 1-113, 1969.
- Flint, E. E., "Design for Photogrammetric Monitoring of a Gabion Wall," Thesis, University of Washington, 1975.
- Galetto, R., "A Photogrammetric Method for Assessing the Displacements Under Stress of Larger Structure Models (Theory). Bollettino de Geodesia e Scienze Affini, Vol. 27, No. 2, p. 185-198, 1968.
- Galetto, R., Bernini, F. and Cunietti, M., "A Photogrammetric Method for Assessing the Displacements under Stress of Large Structure Models (Experimental Applications)," Bollettino di Geodesia e Scienze Affini, Vol. 27, No. 3, pp. 293-316, 1968.
- Gutu, A., "Photogrammetric Measurement Accuracy of Wall Pillar Cracks in Rock Salt Mines," Buletin de Fotogrammetrie, Special Issue, 1972.
- Gherasim, Csc. M., "Contribution a la Theorie de la Restitution Affine," International Archives of Photogrammetry, Vol XV, Part 4, Lisbon, 1964.
- Hallert, B. and Ottoson, L., "General Differential Formulae of the Complete Projective Relations Between Planes," International Archives of Photogrammetry, Vol. XV, Part 4, Lisbon, 1964.



- Hallert, B., "Some Remarks Concerning the Theory of Errors for Convergent Aerial Pictures in Comparison with Near Vertical Pictures," International Archives of Photogrammetry, Vol. XII, Part 4a, Stockholm, 1956.
- Harris, W. D., Tewinkel, G. C., and Whitten, C. A., "Analytical Aerotriangulation," C&GS Technical Bulletin, No. 21, pp. 1-39, 1962.
- Henneberg, H. G., "Das Guri-Projekt und die Vermessung Grosser Sperren," Zeitschrift fur Vermessungswesen, DVW, Vol. 91, No. 11 and No. 12, pp. 385-395, 500-507, 1966.
- Hou, Michael C. Y., "Aerotriangulation Precision Attainable for Highway Photogrammetry," American Society of Photogrammetry and American Congress on Surveying and Mapping 1972 Fall Convention, Columbus, Ohio, October 1972.
- Hou, Michael C. Y., "Are Three Pointings Necessary?," Photogrammetric Engineering and Remote Sensing, 1974.
- Jijina, Cawsie, "A Check of the Stability of the Exterior Orientation Elements in a Terrestrial Camera System," Thesis, University of Washington, 1977.
- Jochmann, H., "Betrachtung zur rechnerischen Bestimmung der Modellpunkte," Vermessungstechnik, Vol. 12, H. 4, Dresden, 1964.
- Karara, H. M. and Marks, G. W., "Analytical Aerial Triangulation for Highway Location and Design," University of Illinois, pp. 1-227.
- Keller, M. and Tewinkel, G. C., "Space Resection in Photogrammetry," C&GS Technical Bulletin No. 32, pp. 1-10, 1966.
- Kenechny, G., "Interior Orientation and Convergent Photography," Photogrammetric Engineering, Vol. XXXI, No. 4, Washington, D. C., 1965.
- Makarovic, B., "Model Deformations and Their Compensational Possibilities in Affine Plotting," I.T.C. Publication A-22, Delft, 1963.
- McNair, A. J., "Photogrammetric Calibration of World's Largest Radio Astronomy Telescope," Computational Photogrammetry Symposium, pp. 1-23, 1969.
- Moren, A., "Summary of Tests of Aerial Photographs of the Oland Test Field," Photogrammetria, Vol. 20, pp. 115-123, 1965.
- Neumaier, K. and Kasper, H., "Aerial Triangulation Text with Super Wide Angle Photography," O.E.E.P.E., Special Publication No. 2. Österreichische Zeitschrift fur Vermessungswesen, Vienna, 1965.
- Ottoson, L., "Adjustment of the Centering of Images in Projectors with the Aid of Fiducial Marks," International Archives of Photogrammetry, Vol. XII, Part 4, Stockholm, 1956.

- Panel Discussion, "The Ballistic Camera Accuracy Review Project," RCA Service Company, Photogrammetric Engineering, Vol. 30, No. 2, pp. 307-311, 1964.
- Planicka, A., "Die Renutzung der Terrestrischen Photogrammetrie in Deformationsmessung von Steinschuttdammen," Paper presented at the 6th Internal Course for Engineering Surveys of High Precision, Graz, Austria, 1970.
- Richardson, J. T., "Measured Deformation Behavior of Glen Canyon Dam," Journal of the Surveying and Mapping Division, Vol. 94, No. SU2, September 1968, pp. 149-168.
- Rinner, K., "Photogrammetrische Auswertung mit hilfe Affiner Modelle," Photogrammetria, Vol. VIII, Nr. 4, Delft, 1951-52.
- Roehm, L. H., "Deformation Measurements of Flaming George Dam," Journal of the Surveying and Mapping Division, A.S.C.E., 1968.
- Rosenfield, G., "The Problem of Exterior Orientation in Photogrammetry," Photogrammetric Engineering, Vol. XXV, No. 4, Washington, D. C., 1959.
- Schoeler, H., "Die Theorie der umgeformten Strahlenbündel und ihre praktische Anwendung im Stereometrograph aus Jena," International Archives of Photogrammetry, Vol. XV, Part 4, Lisbon.
- Schmid, H. H., "Analytical Photogrammetric Instruments," Photogrammetric Engineering, Vol. 30, No. 4, pp. 559-567, 1964.
- Schut, G. H., "Construction of Orthogonal Matrices and Their Application in Analytical Photogrammetry," Photogrammetria, Vol. XV, Nr. 4, Delft, 1958-59.
- Schut, G. H., "Experiences with Analytical Methods in Photogrammetry," Photogrammetric Engineering, Vol. 27, No. 4, pp. 564-570, 1960.
- Sigmark, E., "Some Examples of Application of the Grid Method for the Determination of the Inner Orientation of Terrestrial Cameras," International Archives of Photogrammetry, Vol. XII, Part 4c, Stockholm, 1956.
- Sowers, George B. and Sowers, George F., Introductory Soil Mechanics and Foundations, Third Edition.
- Sun, Lo-jung L., "Photogrammetric Monitoring of a Gabion Wall," Thesis, University of Washington, 1976.
- Taylor, E. A. and Lampton, B. F., "A Report on the Camera Calibration Phase of the C&GS Satellite Geodesy Program," Photogrammetric Engineering, Vol. 30, No. 2, pp. 245-249, 1964.

- Tewinkel, G. C., "Analytic Relative Orientation in Photogrammetry," Coast and Geodetic Survey, 1961, pp. 1-29.
- Torlegard, K., "On the Determination of Interior Orientation of Close-Up Cameras under Operational Conditions Using Three-Dimensional Test Objects," Stockholm, Tryckeri ab Skandia, 100 p., 1967.
- Veress, S. A., "The Effect of the Fixation Disparity of Photogrammetric Processes," Photogrammetric Engineering, Vol. XXX, No. 1, Washington, D. C., 1964.
- Veress, S. A., "Aerial Triangulation Using Independent Photo Pairs," Journal of Surveying and Mapping Division, Proceedings of the American Society of Civil Engineers, New York, 1965.
- Veress, S. A., "Model Deformation and its Effect on Attainable Accuracy," Journal of the Japan Society of Photogrammetry, Vol. 6, No. 7, 1967.
- Veress, S. A., Interim Technical Report Study of the Three Dimensional Extension of Polluted Air, March 1969.
- Veress, S. A., "The Use and Adoption of Conventional Stereoplotting Instruments for Bridging and Plotting of Super Wide Angle Photography," Canadian Surveyor, Vol. XXIII, No. 4, Ottawa, 1969.
- Veress, S. A., "Determination of Motion and Deflection of Retaining Walls, Part I, Theoretical Considerations," University of Washington, Final Technical Report, 1971.
- Veress, S. A. and DeGross, G. E., "Determination of Motion and Deflection of Retaining Walls, Part II, Technical Applications," University of Washington, Final Technical Report, 1971.
- Veress, S. A., Adjustment by Least-Squares, American Congress on Surveying and Mapping, 1974.
- Veress, S. A., "Measures of Accuracy for Analysis and Design of Survey," Surveying and Mapping, December 1973, Vol. XXXIII, No. 4, pp. 435-442.
- Wolf, Paul R., Elements of Photogrammetry, McGraw-Hill, Inc., 1974.
- Yzerman, H., "The S. D. I. a New Method for Stereoscopic Measurements and Plotting," International Archives of Photogrammetry, Vol. XII, Stockholm, 1956.
- Zarzicki, J. M., "Some Theoretical and Practical Problems in Photogrammetric Bridging," Photogrammetric Engineering, Vol. XXI, No. 5, Washington, D. C., 1955.
- Zeller, M., Text Book of Photogrammetry, H. K. Lewis and Co., Ltd, 1952.